ELECTROPLATING METHOD AND ITS APPLICATIONS

HAJIMU ŌKUBO

Department of Mechanical Engineering

(Received Oct. 15, 1959)

ABSTRACT

This is the English translation of the author's study on the electroplating method which was successively published in the Japanese journal "*Kikai no Kenkyū*" during the last several years.[1] The outline of the present paper except the last portion was reported at the *First All-Union Congress on Theoretical and Applied Mechanics of USSR*, Moscow, January 27–February 3, 1960.

Though the matter herein stated, partly, translated in English, was published in several foreign periodicals, the method proposed may be strange to most scientists in other countries who are acting in the field of experimental stress-analysis.

The electroplating method is based on the sensitive colour change on the surface of plated copper made by micro-flecks and also on the grain growth in plated copper, both caused by the reversals of cyclic stress. The method has been applied to examine the stress concentration in shafts containing grooves or holes and has been proved useful for an accurate determination of peak stress.

The method is also favourably applied to the determination of microscopic strain-distribution even in metals having rather small crystal grains.

One promising field of application which will be developed in future is the prediction of fatigue failure which may occur in a machine element under operation. Quantitative determination of peak stress will be possible by this method for the machine element rotating in a closed casing, if more extensive investigation on the nature of flecking be completed in future.

Introduction

Owing to mathematical difficulties a complete theoretical solution for the stress concentration at a section of discontinuity, such as a groove or hole, exists in only a few of the simplest cases, especially in three-dimensional cases. In the majority of cases, informations regarding stress concentration are obtained by experimental stress-analysis. For this purpose various methods of stress measurement, such as the photoelastic method, the brittle-coating method and strainmeters, are usually employed.

It is true that technique has considerably advanced for the photoelastic determination of plane stress and more recently the method has been extended to three-dimensional cases. In three-dimensional cases, however, inevitable error occurring in the measurement perceptively reduces the accuracy of result, since peak stress usually occurs in a minute area on the surface of a specimen.

In using the brittle coating method, it requires high technique to have a coating of uniform thickness if the shape of a specimen is irregular, while the

uniformity of a coating immediately affects results. Moreover, the sensitivity of coatings is keenly affected by various conditions of the coating material, namely, drying time of coating material, atmospheric conditions during the testing period, and many other conditions. Accurate determination of stress can not be expected by means of the brittle coatings though the method is useful for qualitative examination of the stress distribution in structures.

When used strain gauges, either mechanical or electric, technical difficulty arises from the highly localized character of the stress concentration, for an accurate determination of peak strain occurring at a minute area. The shorter the gauge length and the larger the size of specimen, the more accurate will be the determination of the stress at a peak point, provided the gauge has enough sensitivity. There is, however, a certain limit in reducing the gauge length and enlarging the specimen.

The electroplating method which is rather strange to researchers of experimental stress-analysis, has been developed in Japan with the view of measuring the peak stress due to notches. It has been proved useful for an accurate determination of peak stress, since the method is more free from those technical difficulties occurring in the usual method described.

The study on the electroplating method, however, is still on the way of advance and little information is available except a few recent investigations made by Japanese researchers.[1)~11)] Though the method is developed initially with the view of measuring an accurate value of peak stress, applications in many other fields are now promised as will be described later.

Conditions for Deposition and Factors Controlling the Proper Stress

When a copper-plated specimen is subjected to cyclic stress, the surface of the plated copper changes in colour owing to micro-flecks produced by fatigue. These flecks, being produced only in a very thin surface layer of the plated copper, are readily removed by a slight electropolishing.

With increase of the number of cycles, the depth of colour, the thickness and the size of flecks are gradually increased, provided that the magnitude of the cyclic stress is larger than a certain value. The increasing rate is large at a certain value of the cyclic stress which is characteristic of the quality of the plated copper. The quality of plated copper is affected by the surface finish of the basis metal and more keenly by the conditions for deposition, namely, the quality of plating solution, current density, and the temperature during the period of deposition, and also by the heat treatment after deposition.

Every precaution is taken, so as to have the constant quality of the plated copper. The surface of the basis metal is carefully polished before plating with emery-paper of the same mesh, and the conditions for deposition are kept constant throughout the investigation. Specimens used in this experiment are rods of 0.89 per cent carbon steel. They are prepared by treatment in dilute H_2SO_4 and caustic alkali after polishing and then receive a preliminary deposit of copper from a cyanide copper vat.

The conditions for preliminary deposition are as follows:

Solution:	CuCN	23 g
	NaCN	30 g
	Na_2CO_3	10 g
	H_2O	1000 cc

Current density: 0.06 amp/dm^2; temperature: 30°C; bath voltage: 0.35 V; duration of deposition: 20 min.

The usual conditions for additional deposition are as follows:

Solution:	$CuSO_4 \cdot 5\,H_2O$	250 g
	H_2SO_4	80 g
	H_2O	1000 cc

Current density: 3 amp/dm^2; temperature: 23°C; bath voltage: 0.5 V; duration of deposition: 15 min.

The thickness of the plated copper is almost 0.01 mm for the current density and the duration for deposition described. It is one-twentieth of the usual thickness of a brittle coating. It is well ascertained that the thickness of plated copper does not affect the result perceptively.

To avoid the disarrangement in the results, special precaution is taken to eliminate the difference in the quality of plating solution. For this purpose, a plenty of plating solution of the same quality is prepared at a time and every specimen is always plated by a new plating solution, since the plating solution is made with commercial grade copper-sulfate without any preliminary treatment for purification. Specimens used in one experiment are plated at a time and are stored in a deciccator until the test. The preservation for several weeks does not affect the results.

For abbreviation, the limit value of cyclic stress within which the flecks are not produced by fatigue is termed "proper stress" of the plated copper for an assigned number of repetitions of cyclic stress. The value of proper stress, however, is a nominal one and is not the real value of cyclic stress arising in the plated copper. It is based on the elastic moduli of the underlying steel, since the value is usually derived from the bending moment or twisting moment acting on a specimen. The variation in the appearance of flecks, which is due to the change of cyclic stress, is very sensitive at a proper stress, so an accurate estimation of the surface stress is feasible by observing the appearance of flecks.

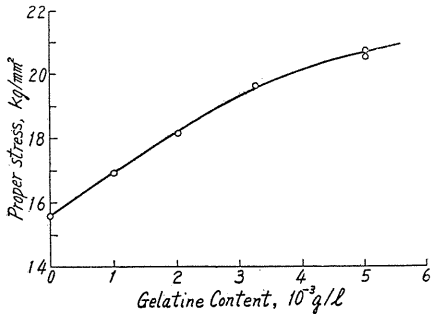

FIG. 1. Relation between proper stress and gelatine content in plating solution.

Every factor effecting the proper stress is not known at present, but the most remarkable one among the known factors is the impurity contained in the plating solution. A very small quantity of gelatine contained in the plating solution, considerably raises the value of proper stress, as is shown in Fig. 1. Another notable

one is the effect of heat treatment. The higher the temperature and the longer the duration of heat treatment, the reduction of the proper stress is more perceptible. But when a specimen is annealed at a higher temperature than 300°C, the process of recrystallization of copper being advanced, the flecking does not occur by cyclic stress.

Process of Producing Flecks

Figure 2 is a test piece of tapered rod partially changed in colour by cyclic stress. Examining the surface of such specimen by microscope, microgroups of fine flaws mixed among the flecks are found and these flaws run almost parallel to the planes of maximum shear. Figure 3 is a micrograph of the flaws produced on the surface of the specimen by rotary bending test; Fig. 4 a micrograph of the flaws produced by torsion test; arrow lines indicate the axial direction of specimens. Close examination shows that a fleck is not a mass of flaws and the group of flaws is not always situated exactly in a fleck. When the specimen is exposed to a flow of hydrogen gas at 300°C during the comparatively short interval of 5 min, the flecks disappear, leaving only a trace, while the groups of flaws suffer no change whatever. Figure 5 is an original fleck and Fig. 6 its trace deoxidized by a flow of hydrogen gas. When the specimen is exposed to a flow of carbon dioxide at the same temperature, the flecks suffer no change. This indicates that they are produced by a chemical change occurring in the surface layer of the plated copper.

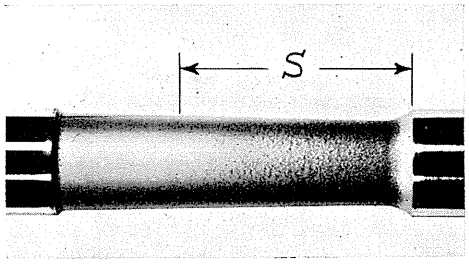

FIG. 2. Test piece partially changed in colour.

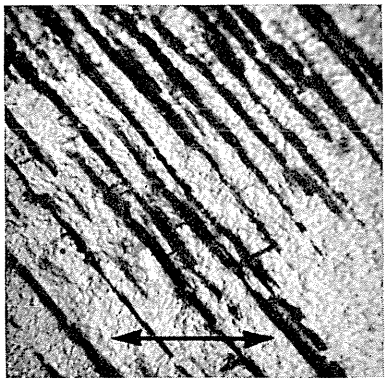

FIG. 3. Flaws, rotary bending (800×).

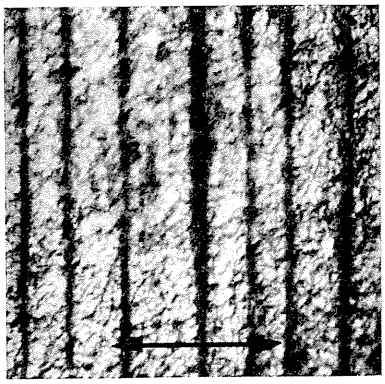

FIG. 4. Flaws, torsin (800×).

Microscopic examination of the surface and cross section of a specimen having been colour-changed, electropolished, and etched, reveals the nature of grain growth in the plated metal. Figs. 7 and 8 are the surface and the cross section of the specimen showing the initial status of grain growth where the number of

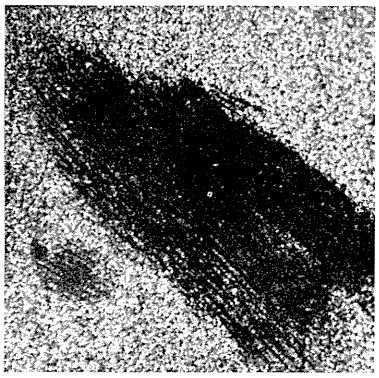

FIG. 5. Fleck, before deoxidation (260×).

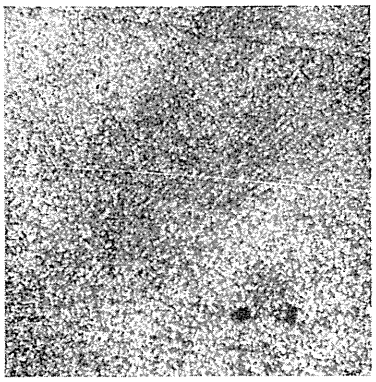

FIG. 6. Fleck deoxidized in hydrogen gas (260×).

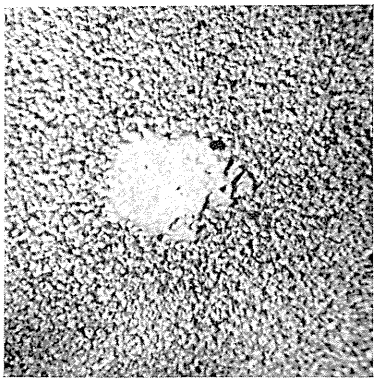

FIG. 7. Initial status of grain growth, after direct stress of ±18 kg/mm² for 9×10^5 cycles (800×).

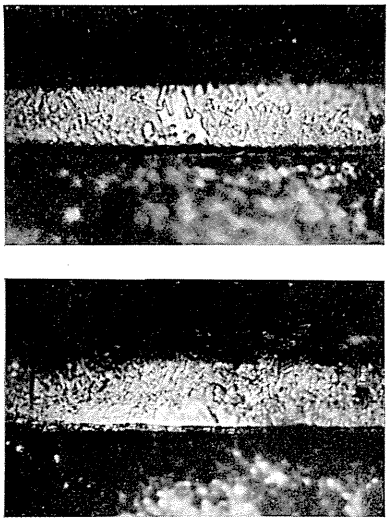

FIG. 8. Initial status of grain growth, after direct stress of ±18 kg/mm² for 9×10^5 cycles (800×).

repetitions of cyclic stress is below one million, the flecks do not appear as yet, and the surface of the specimen does not change in colour, while the physical change as shown in the figures is already found in the plated metal. With sufficient increase in the number of repetitions of cyclic stress, the grains grow up to the surface of the plated metal, as shown in Figs. 9 and 10, and the flecks are produced.

The grain growth usually starts from the boundary of the two plated-coppers which are considerably different in grain size, namely from the boundary of the preliminary and additional plated-coppers. The original grain sizes of the former and the latter are of the order of 0.3 μ and 1 μ, respectively, Figs. 11 and 7. The physical change described occurs in the latter only and not in the former.

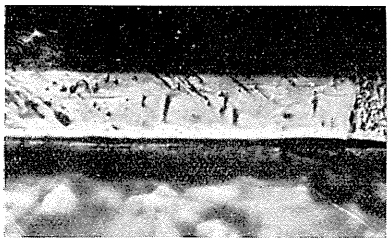

FIG. 9. Grown grain, after direct stress of ± 18 kg/mm^2 for 5×10^6 cycles ($800\times$).

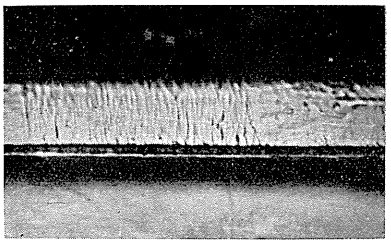

FIG. 10. Grown grain, after direct stress of ± 20 kg/mm^2 for 5×10^6 cycles ($800\times$).

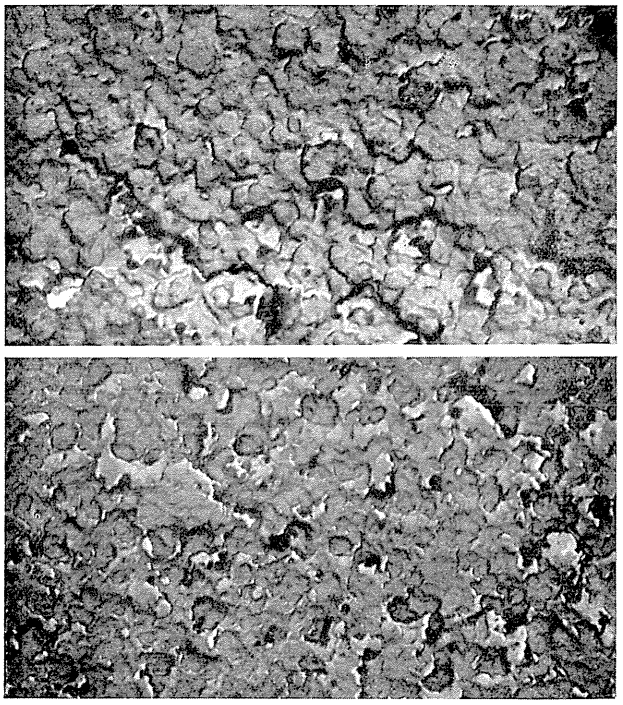

(a)

(b)

FIG. 11. Surface view of underlying plated-copper ($12000\times$) (a) before stressing, (b) after stressing.

This shows that the grain growth resulting in flecking, is originated by the mutual action between the two plated-coppers rather than the mutual action between the plated copper and the basis metal, since the additional plated-copper is isolated from the basis metal by the preliminary plated-copper which suffers no change. The surface views of the preliminary plated-copper, before and after stressing, are shown in Fig. 11. From the figure one can hardly find any change in physical constitution occurred on the surface of the preliminary plated-copper.

Figs. 12 and 13 are micrographs, the former of a fleck and the latter of a figure on the etched surface after slight electropolishing. By means of etching,

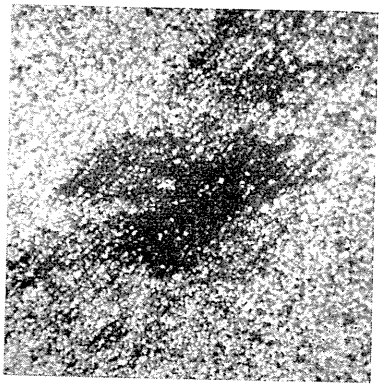

FIG. 12. Fleck (260×).

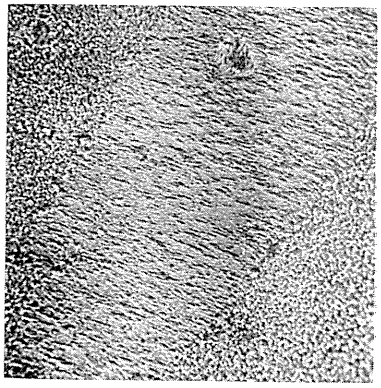

FIG. 13. Etched figure after electropolishing, showing a grown grain and the neighbouring micrograins (260×).

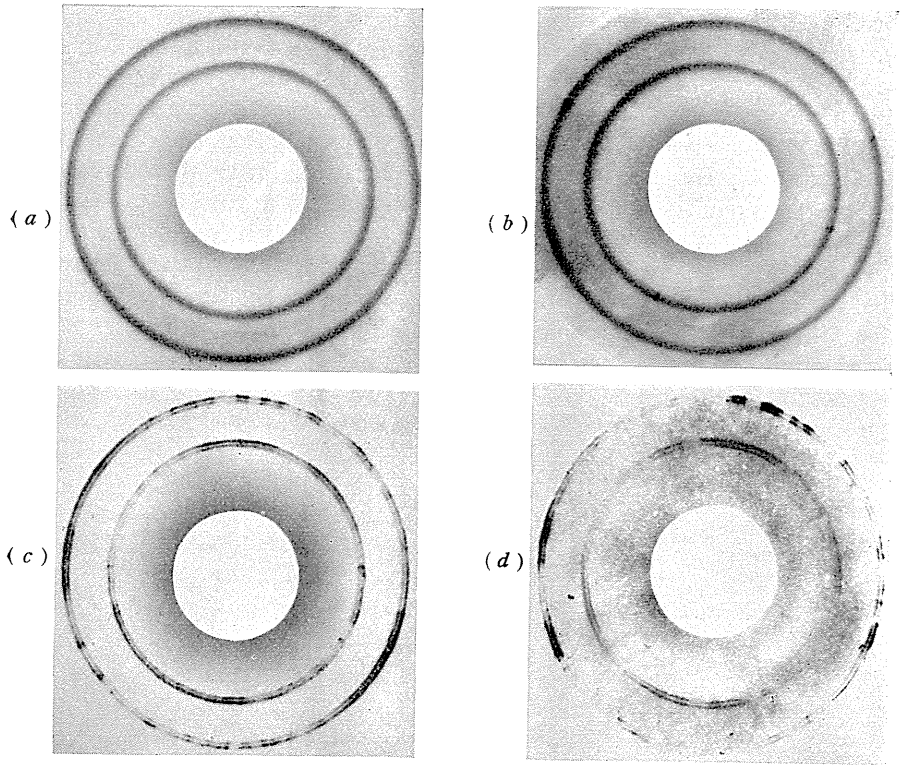

FIG. 14. X-ray patterns

(*a*) before stressing, (*b*) after direct stress of ± 20 kg/mm^2 for 2×10^6 cycles, (*c*) after direct stress of ± 22 kg/mm^2 for 5×10^6 cycles, (*d*) after direct stress of ± 22 kg/mm^2 for 16×10^6 cycles.

one can easily distinguish the part changed in physical constitution from the remaining part, namely, a large grown-grain from the neighbouring micrograins.

Comparison of the X-ray patterns at several stages of stressing, shown in Fig. 14, also suggests grain growth in the plated metal.

These results show that, when a specimen plated with copper is submitted to reversals of cyclic stress, if the magnitude of the stress exceeds the proper value, some of the micrograins in the additional plated-copper gradually grow at the boundary of the underlying plated-copper. With increase of the number of repetitions, the grains grow up to the surface of the plated metal. Then faint flecks are produced thinly. The grains, however, grow to a considerable size with sufficient increase of the number of repetitions, and the size, the depth of colour and the thickness of the flecks are all increased, and the microgroups of fine flaws appear on the surface of these grown grains.

The size of grown grains is, in general, almost equal to the size of flecks. It is considerably affected, however, by various conditions even though the same ground steel is used, for example by a slight difference of plating solution, by the temperature of deposition, by the heat treatment of specimens and other factors. The size of grown grains is much smaller when the plating solution is made with cupric oxide instead of commercial copper sulfate, when the temperature of deposition is much higher than room temperature, and when specimens are annealed at a lower temperature than 300°C.

In cases where the size of grown grains is quite small, the grain growth and the flecking generally occur at a lower value of cyclic stress than usual and the value of proper stress is appreciably reduced. The microgroups of fine flaws described usually are not found in this case. The reduction of proper stress is perceptible even for the treatment at the temperature lower than 100°C, if the duration of treatment is sufficiently long. Fig. 15 is a surface view showing grown grains in the plated metal when the plating solution is made with cupric oxide. Figs. 16 and 17 are surface views showing the constitution of the plated metal before and after stressing, respectively, when the specimen is annealed at 150°C for 1 hr in vacuum. Comparing Figs. 15, 17 and 13, it would appear that the size of grown grains becomes much smaller than in the usual case. Figs. 18

FIG. 15. Grown grains, plating solution made with cupric oxide (260×).

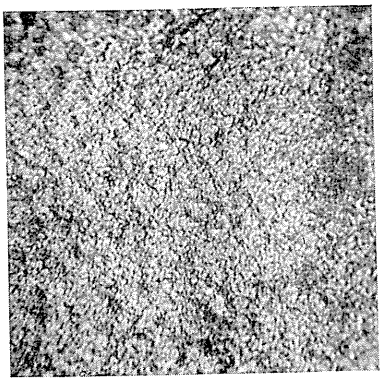

FIG. 16. Annealed at 150°C, before stressing (800×).

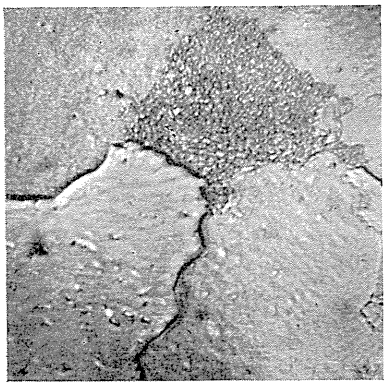

FIG. 17. Annealed at 150°C, after stressing (800×).

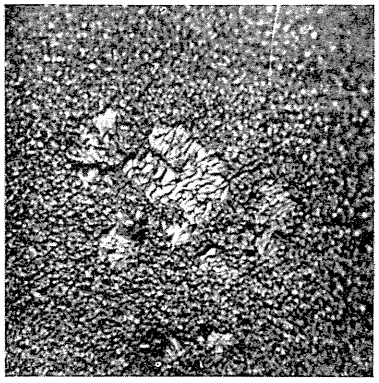

FIG. 18. Annealed at 250°C, before stressing (800×).

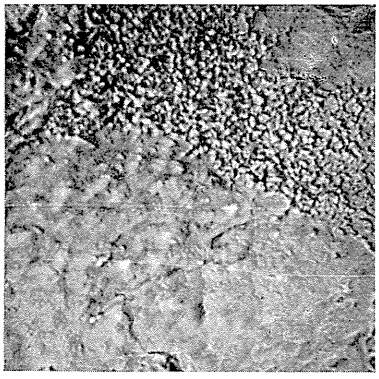

FIG. 19. Annealed at 250°C, after stressing (800×).

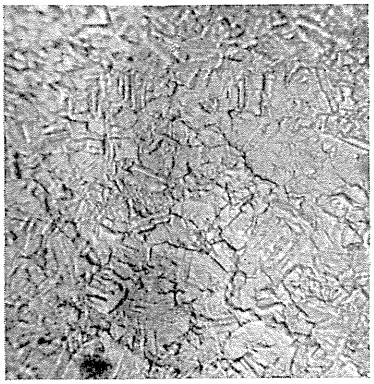

FIG. 20. Annealed at 350°C, before stressing (800×).

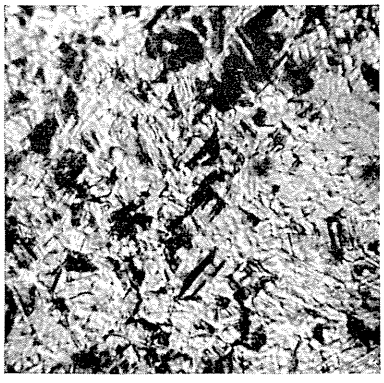

FIG. 21. Annealed at 350°C, after stressing (800×).

FIG. 22. Annealed at 600°C, before stressing (800×).

and 19 show the surface of plated metal annealed at 250°C. As is shown in Fig. 18, the recrystallization of copper occurs in part by the heat treatment.

Figs. 20 and 21 show the surface of the plated metal annealed at 350°C before and after stressing, respectively. In this case, since the progress of recrystallization of copper is considerably advanced, the grain growth caused by cyclic stress does not occur and the flecks described are not produced. The surface of a specimen submitted to cyclic stress, however, becomes tarnished owing to the appearance of microflaws, as shown in Fig. 21.

Figs. 22 and 23 are views of the surface and cross section of the plated metal annealed at 600°C, where the recrystallization of copper is complete. The endurance limit of annealed copper[12] almost agrees with the real value of the proper stress of the plated copper. Consequently, when the magnitude of the cyclic stress passes the proper stress, fatigue cracks, as shown in Fig. 24, appear instead of the flecks.

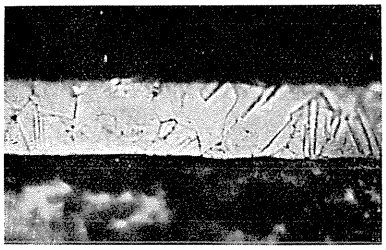

FIG. 23. Annealed at 600°C, before stressing (800×).

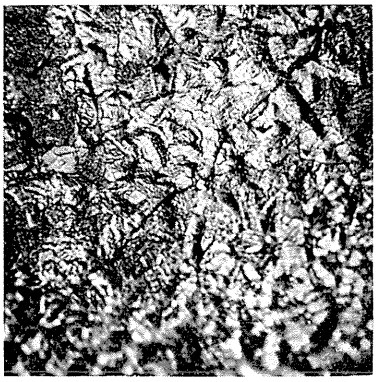

FIG. 24. Annealed at 600°C, after stressing (800×).

Stress-Concentration Factors in Shafts

Determination of proper stress A preliminary test is made to determine the proper value of shearing stress below which flecks are not produced by fatigue. Test pieces used for the torsion fatigue test are conical rods of carbon steel with dimensions as shown in Fig. 25. For test pieces, the use of slightly tapered rods is favourable in this experiment, since the appearance of flecks varies continuously along the length of the rod according to the change of the surface stress, so we may have the status of flecks corresponding to a certain range of stress by a test. If we measure the distance S from one end to the

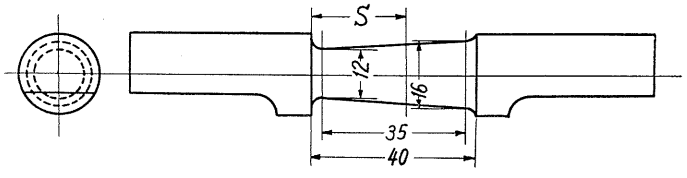

FIG. 25. Dimensions of test piece in millimeter.

TABLE 1. Determination of Value of Proper Stress

No. of test piece	Torque (kg-m)	S (mm)	τ_p (kg/mm²)	Mean value of τ_p (kg/mm²)
1	±3.48	12.0	±7.90	±7.88
2	±3.44	11.8	±7.85	
3	±4.26	19.4	±7.86	
4	±3.48	11.9	±7.92	

point corresponding to the proper stress, the value of the proper stress is immediately calculated from the elementary torsion formula for circular shafts, since the torque acting on the rod and its diameter at S can be measured.

The results thus obtained are given in Table 1, the number of repetitions of the cyclic stress being taken 5×10^6. From the table we take for the proper stress in shear, the value

$$\tau_p = \pm 7.88 \text{ kg/mm}^2.$$

Fig. 26 is the micrograph of flecks whose status around the vertical line shows the typical one for the proper stress. Fig. 27 shows a test piece of the normal type, usually used in torsion fatigue test, so that the radius of fillet is taken large enough for the usual test. However, by the electroplating method, the slight stress-concentration at the fillet is apparent as is shown in the figure.

In order to find which stress predominates the flecking, proper stress was determined both in torsion and bending, using the plating solution of the same quality prepared for the particular test. The proper value of direct stress was obtained by means of rotary bending test. The process of determining the proper stress, however, is quite similar to that employed in torsion. The results are as follows:

In torsion, the averaged value through two tests is $\tau_p = \pm 8.0$ kg/mm². In bending, the direct stress averaged through three tests is $\sigma_p = \pm 15.4$ kg/mm², and the shearing stress corresponding to the direct stress in a uniform tension field is $\tau_p = \frac{1}{2}\sigma_p = \pm 7.7$ kg/mm². The values of proper stress in shear, measured in two different types of loading, are in fairly good agreement. This shows that shearing stress can be used for the criterion of producing flecks without perceptible error, even when a specimen is under biaxial stress. Consequently, in general, the physical change in the constitution of the plated copper can be attributed entirely to the reversals of shearing strain. It has heen reported that the shearing strain in the plated copper corresponding to the proper stress is always about $\pm 1\times10^{-3}$ both in torsion and bending, irrespective of the basis metal.[7]

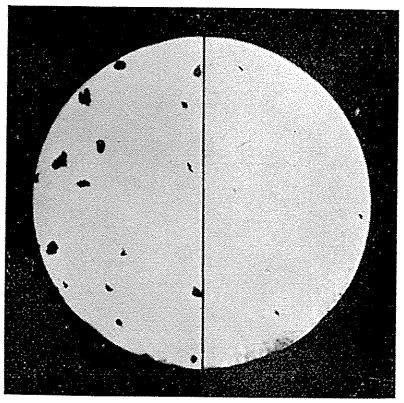

FIG. 26. Typical status of flecks at proper stress (25×).

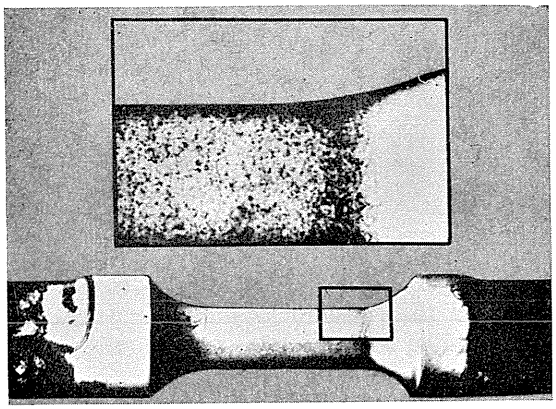

FIG. 27. Test piece used in usual fatigue tests.

Shaft with a transverse hole, torsion In a shaft with a transverse hole, places where the stress concentrates are not presumed precisely from the usual knowledge of elasticity. To locate these places, a preliminary test was made for the specimen as shown in Fig. 28. The illustration shows colour change in several places caused by cyclic stress. On the outer surface of the specimen, the stress concentrates at four points, marked by m in the figure, in the neighbourhood of the hole edge. In the bore, however, the stress concentrates at eight points marked by n, at a small distance below the edge of the hole. When the ratio d/D is comparatively small, the stress at the latter is much larger than that at the former, so fatigue cracks always start from the latter. Fig. 29 shows the fractured surface of the specimen. It shows a clear aspect for the stress concentration and also for the crack started from the peak point n.

Having determined the peak points, further test was carried out to obtain stress-concentration factors in shafts with transverse holes of various diameters.

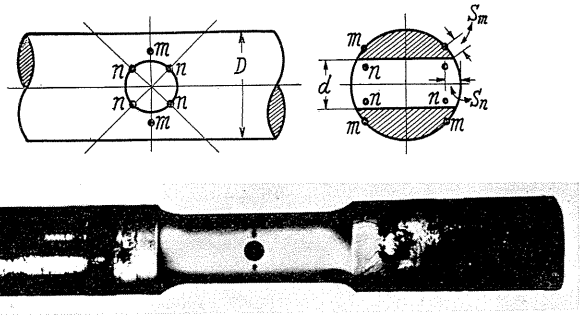

FIG. 28

FIG. 28. Test piece with transverse hole, changed in colour at peak points.

FIG. 29

FIG. 29. Fractured surface of specimen with transverse hole.

Test pieces used are 20 mm diameter with a transverse hole in each, diameters of which are 2.1, 3.6 and 5.1 mm, respectively.

The torques which produce proper stress at m and n for 5×10^6 cycles of stress are measured by observing the surfaces of specimens and bores with a microscope. The status of flecks at m or n, corresponding to the proper stress, is assumed to be in such condition that faint flecks appear in some of the cognate points (m or n) but never appear in them for a slightly smaller stress. The torques which produce the proper stress at m and n are denoted by T_m and T_n, respectively, and are shown in Table 2. For an accurate determination of T_n, a satisfactory observation in the bore is required. For this purpose, in some instances, test pieces are planed through the axis of a hole, according to the requirement in observation.

The stress-concentration factor usually is given by the ratio of the maximum stresses in two shafts of the same diameter, with and without a hole, which are subjected to equal torques. This is equal to the inverse ratio of torques which produce the same maximum stress in either shaft. The torque which produces the proper stress (kg/mm^2) on the surface of the shaft, 20 mm diameter and without a hole, is $(\pi/2)\tau_p$ kg-m. Thus we have

$$K=\frac{\pi\tau_p}{2T}, \tag{1}$$

where T is the torque producing the proper stress at a peak point and K is the stress-concentration factor. The values of K in the bore (n) and at the hole

TABLE 2. Determination of Torque to Produce Flecks at Peak Points of Shafts with Transverse Holes

Diam of hole (mm)	Torque (kg-m)	Flecks produced at		T_m (kg-m)	T_n (kg-m)
		m	n		
5.1	±6.03	Some points	All points	±5.87	±5.11
	±5.87	Some points	All points		
	±5.77	No points	All points		
	±5.12	No points	Some points		
	±5.11	No points	Some points		
	±4.93	No points	No points		
3.6	±6.66	Some points	All points	±6.66	±5.44
	±6.44	No points	All points		
	±6.32	No points	All points		
	±5.85	No points	All points		
	±5.75	No points	All points		
	±5.58	No points	Some points		
	±5.46	No points	Some points		
	±5.44	No points	Some points		
	±5.38	No points	No points		
2.1	±7.62	Some points	All points	±7.62	±5.71
	±7.44	No points	All points		
	±7.21	No points	All points		
	±6.79	No points	All points		
	±5.97	No points	All points		
	±5.71	No points	Some points		
	±5.56	No points	No points		
	±6.40	No points	No points		

TABLE 3. Location of Maximum Stress and Value of Stress-Concentration Factors

Diam of hole (mm)	d/D	S_m (mm)	S_n (mm)	T_m/T_n	K	
					In bore (n)	At hole edge (m)
2.1	0.105	0.6	0.4–0.5	1.33	2.17	1.63
3.6	0.180	1.1	0.5–0.8	1.22	2.28	1.86
5.1	0.255	1.6	0.8–1.1	1.15	2.42	2.11

edge (m), calculated from the foregoing relation, are shown in Table 3, together with S_m and S_n, the rough locations of the peak points, m and n. As is shown in the table, S_m and S_n decrease with the decrease of d/D, and the ratio T_m/T_n is likely to approach almost 1.5 when the diameter of hole becomes infinitely small. This shows that the normal stress at n is three times the shearing stress at m, since the criterion of producing flecks is shearing stress. This result for infinitely small holes agrees with the theoretical one previously derived by Neuber.[13] In the range of the diameter of hole treated here, the stress at n is always larger than that at m, but the stress at m, also becomes effective when d/D is large enough, since the ratio T_m/T_n decreases with increase of d/D.

The stress-concentration factors in the bore have been derived by Seely and Dolan by means of the plaster-model method.[14] From Table 3, the values of K both in the bore and at the hole edge are plotted in Fig. 30, together with their results represented by a dashed line. The latter shows averaged values through 5–8 tests, and the deviation of each value from the mean is about 10 per cent for every size of hole. As is shown in the figure, their data for small holes are much smaller in comparison with those obtained here as well as theoretically presumed values.[13] Recent investigations by means of strain gauges were published for similar cases by Thum, Kirmser and Seeger, respectively.[15] The results derived by them are considerably larger in comparison with those obtained here. The author doubts, however, whether the stress-concentration factors are derived in the ratio of the maximum direct stress to the nominal shearing stress. If this difference for the derivation of K be taken into account, their data are much smaller in comparison with those derived here. Their results that, in a certain range of small d/D, K decreases with the increase of d; namely, the greatest strength for a shaft is obtained by making the diameter of the hole to a suitable size.

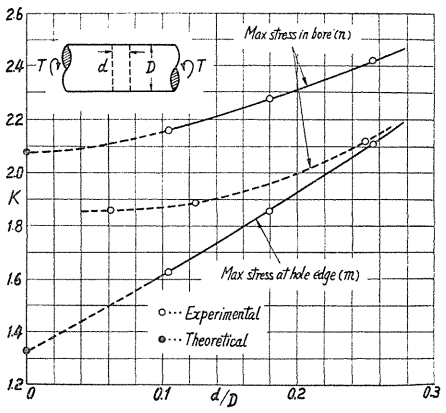

FIG. 30. Stress-concentration factors in shafts with transverse holes, submitted to torsion.

The same conclusion would be derived from other experimental results obtained previously by various

writers for shafts with transverse holes submitted to bending or torsion.[16] Such a conclusion, however, is quite contrary to the usual practice which tends to make a shaft with the smallest possible size of hole the strongest one. The author rather inclines to conclude that the usual method for stress measurements such as the freezing method and the use of strain gauges are not suitable for an accurate measurement of the stress concentration in shafts with small transverse holes.

As was described, the substantial effect of direct stress in producing flecks is 8.0/15.4 times that of shearing stress. Consequently, if the maximum direct stress in the bore be four times the nominal shearing stress, which is Neuber's theoretical value for infinitely small holes, the stress-concentration factor observed by the present method will be $4\times 8.0/15.4=2.08$, and the curve of K, in the bore, must pass the point $d=0$, $K=2.08$, as is indicated by the dashed curve in Fig. 30. The curve of K, at the hole edge, may be extended to the theoretical value 4/3 at $d=0$, as is shown in the same figure.

Shaft with a transverse hole, bendng The stress concentration arising from bending is investigated in the same manner. Test pieces used are 15 mm diameter with transverse holes, the diameters of which vary from 1.01 mm to 5.06 mm. The stress-concentration factors both in the bore n and at the edge of the hole m, Fig. 31, are obtained for the mentioned values of the hole diameter. The bending moment which produces the proper direct stress σ_p (kg/mm^2) on the surface of the shaft, 15 mm diameter and without a hole, is 0.331 σ_p kg-m. If M denotes the bending moment which produces the proper stress at m or n, the stress-concentration facter at the point is

$$K=0.331\frac{\sigma_p}{M}\cdot \qquad (2)$$

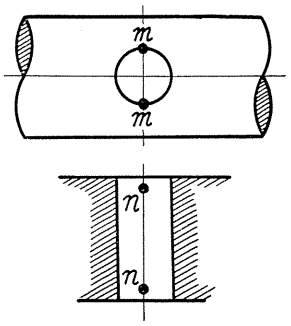

FIG. 31. Locations of peak points.

The results are given in Fig. 32. As is shown in the figure, with decrease of the hole diameter, the two curves of stress-concentration factors both approach the theoretical value 3 for an infinitely small hole in a tension field. The results of various previous investigators derived by different techniques, such as photo-elasticity, mechanical strain gauges, and plaster models, are also shown in the same figure.[14)~16)] Their results are perceptively different from those herein obtained and they all indicate that there is a rapid fall in the value of the stress-concentration factor as the hole diameter is increased from zero as occcurred in torsion.

It is interesting, however, to note that the results of Peterson and Wahl are in agreement with those herein obtained within the discrepancy of several per cent. Furthermore, the curve connecting their experimental points runs almost parallel to the present one, as is indicated by a dashed line in Fig. 32.

The strain figures in the bore and at the hole edge formed by flecking for

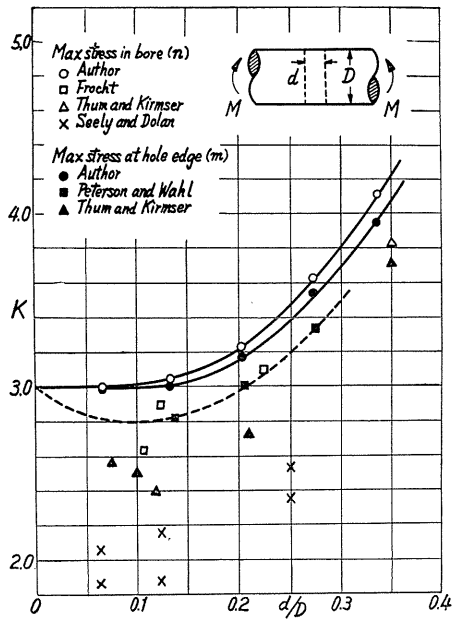

FIG. 32. Stress-concentration factors in shafts with transverse holes, submitted to bending.

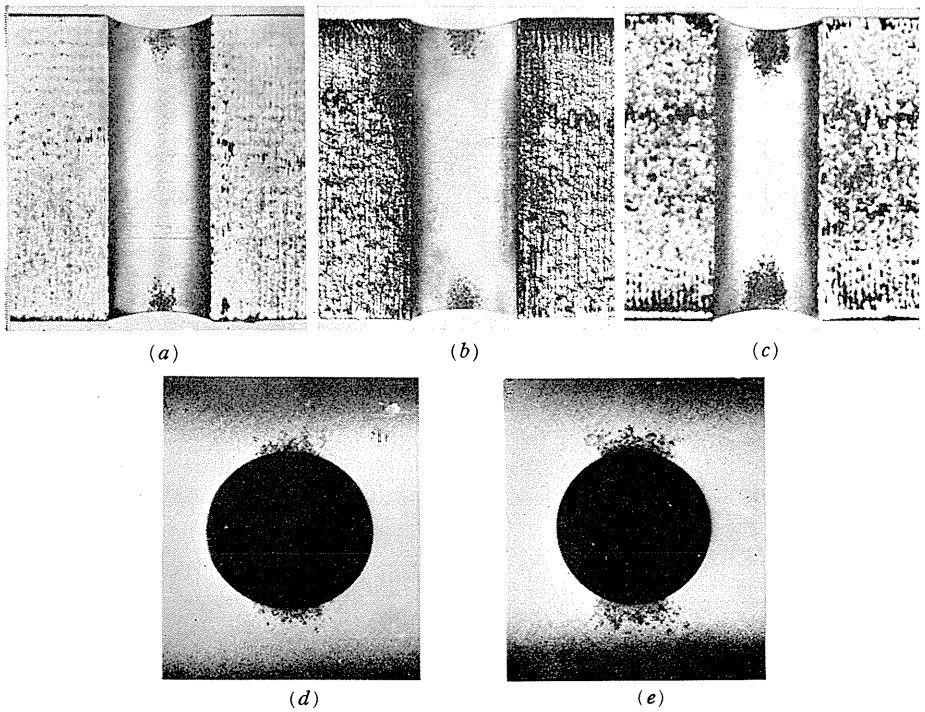

FIG. 33. Strain figures at hole edge formed by flecking; (*a*) $\sigma = \pm 5$ kg/mm^2, (*b*) $\sigma = \pm 6$ kg/mm^2, (*c*) $\sigma = \pm 7.5$ kg/mm^2, (*d*) $\sigma = \pm 7.5$ kg/mm^2, (*e*) $\sigma = \pm 8.5$ kg/mm^2.

5×10^6 cycles of stress are illustrated in Fig. 33. The values of direct stress described underneath each figure are the nominal stress based on the full section of the shaft.

Shaft with a circumferential groove, torsion Tests were made in the manner already described, for shafts of the diameter 20 mm with a circumferential groove in each. The dimensions of notches are given in Fig. 34. To have accurate dimensions of grooves, they are checked by plate gauges which have been measured carefully by a Zeiss comparator. The torque corresponding to the proper stress at the base of groove is found by taking the mean values of torques, corresponding to the two appearances of flecks at the base of groove, one of which is very thin and the other indistinct. The stress-concentration factors calculated from (1) are given in Table 4.

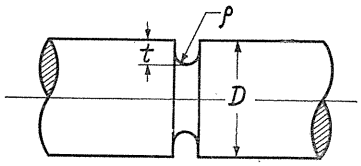

FIG. 34. Dimensions of notches, $D=20$ mm, $\rho=2$ mm, $t=1.5$ mm, 2 mm, 3 mm, 4 mm.

TABLE 4. Value of Stress-Concentration Factors, $D=20$ mm, $\rho=2$ mm

Depth t (mm)	1.5	2.0	3.0	4.0
K	2.6	3.1	4.5	6.9

The formulas for the estimation of stress-concentration factor, where the depth and the radius of a notch are prescribed, have been derived by several previous writers for convenience of practical use.[17] They hold exactly, except Sonntag's formula, in the extreme case where the dimensions of a notch are infinitely small in comparison with those of the shaft. According to the deriving process for the formulas, however, it is obvious that these formulas do not exactly hold for moderate dimensions of a notch, which are likely to be those of practical importance. In the previous paper, the author pointed out that for the particular case of a semi-circular notch the author's formula agrees most closely with the exact values given by Willers[18] in the range of moderate dimensions of the notch and that the formula obtained by Sonntag comes next to the author's.[19] These two formulas for the stress-concentration factor are as follows;

$$\text{Author's} \qquad K=\frac{1+(t/\rho)^{1/2}}{(1-t/a)^2}, \tag{3}$$

$$\text{Sonntag's} \qquad K=\frac{a^2(a-t+\rho)^2(t+\rho)+a^2\rho^2(t-\rho)}{\rho(a-t)^3(a-t+2\rho)}, \tag{4}$$

where a is the radius of the shaft at the cylindrical part and t, ρ represent the depth and radius of a notch, respectively. The values of K, given by these formulas, almost agree in the particular case of a semi-circular notch. But they become considerably different with the increase of the ratio of t to ρ. The discrepancy for large value of t/ρ, is too large even for practical use, and yet theoretical justification for the two would not be easily found, since the two for-

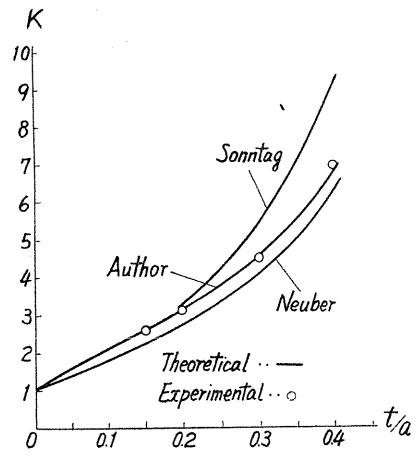

FIG. 35. Relation between the stress-concentration factor and the depth of notch, $\rho=0.2\,a$.

mulas are approximate ones, derived from somewhat different assumptions, respectively. Accordingly, the experimental data obtained in this paper may be a good reference for the justification of the two formulas. The value of K taken from Table 4, together with those calculated from equations (3) and (4), are shown in Fig. 35. It may be seen from the figure that the experimental results herein obtained are in good agreement with theoretical ones, calculated from the author's formula. This indicates that the author's formula is also valid in cases of $t \neq \rho$. In order to investigate the safe range of the formula for the dimensions of groove, we rewrite the formula (3) into the form

$$k = \frac{1+\sqrt{t/\rho}}{1+2\,t/d}\,, \tag{5}$$

in which k is the stress-concentration factor based on the minimum diameter of the shaft, d.

The formula (5) apparently fails in the limit case of infinitely large ρ/t, since the formula gives the value of k less than unity. Moreover, two curves of k for different values of t/ρ derived from the formula actually intersect at a certain value of ρ/d. To eliminate these conflicts and extend the useful range of the formula, we make the following assumption regarding the use of the formula.

Consider two notches of the equal base-radius ρ, the depth of one is slightly larger than the other. If we denote the stress-concentration factors and the depths of the two notches by k_1, k_0, $t+\varepsilon$ and t, respectively, we have

$$k_1 - k_0 = \frac{1+\sqrt{(t+\varepsilon)/\rho}}{1+2\,(t+\varepsilon)/d} - \frac{1+\sqrt{t/\rho}}{1+2\,t/d}\,,$$

where ε is a very small positive quantity. From the relation it follows that

$$k_1 \gtrless k_0 \qquad \text{according as} \qquad \rho/d \gtrless \frac{1}{2\sqrt{t/\rho}\,(2+\sqrt{t/\rho})}\,.$$

Accordingly, the two curves of k for the notches intersect at the point

$$\rho/d = \frac{1}{2\sqrt{t/\rho}\,(2+\sqrt{t/\rho})}\,. \tag{6}$$

We assume that the value of k_1 is replaced by k_0 for the value of ρ/d larger than the value given by (6). Plot the curves of k, taking t/ρ as a constant in

each, and consider the envelope for the family of the curves, then the formula (5) can be used without any conflict at all points on these curves to the extent of ρ/d, at which these curves touch the envelope. For still larger values of ρ/d, however, from the assumption mentioned above, the values of k is taken on the envelope instead of on these curves. The equation of the envelope is readily found from (5), as

$$8\,k(k-1)=d/\rho. \tag{7}$$

This use of the formula, the conflict described being eliminated, considerably extend the validity of the formula. The assumption herein employed, in effect, is that when ρ/d is fixed, the value of k remains constant by the variation of t/ρ provided that ρ/d is larger than a certain value. Formerly Jacobsen obtained the stress-concentration factor in a shaft containing a fillet by using an electrical analogy.[20] His results show that when ρ/d is fixed, k increases with the increase of t/ρ, but remains almost constant by the variation of t/ρ for ρ/d which is larger than a certain value. For instance, the ratio between k for $t/\rho=1$ and for infinitely large t/ρ is 0.87 when $\rho/d=0.075$, but this ratio becomes 0.95 when $\rho/d=0.125$. This shows that the ratio approaches unity when ρ/d becomes large enough. The experimental results for the shafts with fillets can be the background of the assumption described.

For an infinitely large value of ρ/d, k is found from (7) instead of (5), and it follows that the effect of the notch entirely disappears.

The stress-concentration factors for various values of ρ and t are calculated from (5) and (7), and presented by curves in Fig. 36 for convenience of practical use. The corresponding values of k, based on Sonntag's results, which are still referred to in practice,[21] are also shown by dashed lines in the same figure. We find a considerable discrepancy between the values of k herein recorded and those now used in practice.

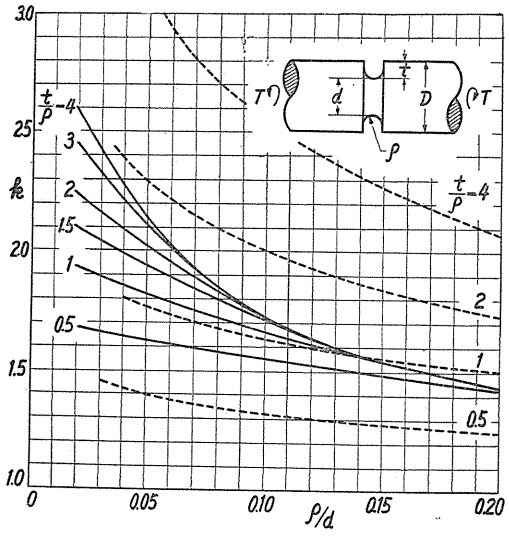

FIG. 36. Relation between the stress-concentration factor and the depth and radius of notch.

To verify the results shown in Fig. 36, two different notches are considered, one is $t=2\rho$, $\rho=0.167\,d$ and the other $t=\rho$, $\rho=0.167\,d$. The measured values of k for the two, obtained by the electroplating method, are 1.49 and 1.47, respectively, while the values of k taken from the curves in Fig. 36 are 1.50 for either notch, so the results shown in the figure are sufficiently accurate for practical use.

Sonntag's formula has been quoted in text books of former edition and still often used for the computation of k in practice, but since his results are in poor agreement with those of other investigators, Neuber's solution is now more generally used.

Neuber's formula for infinitely deep hyperbolic notches is

$$k=\frac{3(1+\sqrt{d/2\,\rho+1})^2}{4(1+2\sqrt{d/2\,\rho+1})}\,. \tag{8}$$

The above formula, however, often gives much smaller values as compared to those obtained here. For instance, in the case of a semi-circular notch of $\rho=d/8$, the exact value by Willers is $k=1.57$, and the experimental value by the author is $k=1.59$, while his formula gives much smaller value of $k=1.44$. Comparing these figures for k, a question arises in connection with the suitability of his solution of deep hyperbolic notches for an accurate evaluation of the stress-concentration factor of a parallel-sided U-notch.

His solution for moderate values of t, based on an interpolation between two limiting solutions gives still smaller values of K, as shown in Fig. 35.

Furthermore, his solution gives a small value of k which almost agrees with Jacobsen's result for a fillet obtained by means of electrical analogy,[20] *e.g.*, his solution gives $k=1.58$ for $\rho/d=0.078$, $t/\rho=4$, while the corresponding value for a shaft containing a fillet is 1.53. Those theoretical and experimental results of other investigators all indicate that his solution gives a much smaller value than the substantial one. Exceptionally, photoelastic results found by the stress freezing method agree with Neuber's results.[22] From which, however, one can hardly conclude the high accuracy of his solution, because photoelastic results in three dimensions are not so accurate as in two dimensions, and it is reported that a considerable measuring error is found in some instances.[23]

His another solution for a flat tension bar with deep hyperbolic-notches also gives, in some instances, slightly smaller values of k even compared to those for semi-circular notches, obtained by photoelasticity,[24]

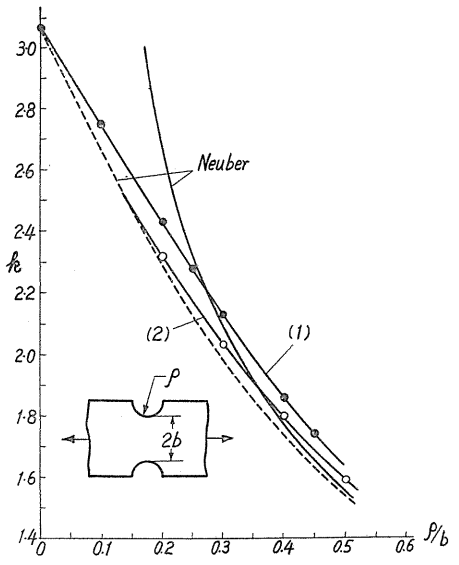

FIG. 37. Stress-concentration factors in flat tension-bars containing semi-circular notches, (1) exact values by Isida, (2) measured values by Frocht.

and his solution for semi-circular notches is always smaller than the observed values, as is shown by a dashed line in Fig. 37. While the measured values of k are perceptively smaller than the accurate theoretical values shown in the same figure.[25]

Shaft with a circumferential groove, bending In so far as the author is aware, little information is available as to the magnitude of the stress-concentration factor for a circumferential groove in a shaft submitted to bending. One notable exception is the analytical results for hyperbolic grooves given by Neuber.

Test pieces used are 15 mm diameter with circumferential grooves of 1.59 mm base radius. The depths of the grooves vary from 1.01 mm to 3.18 mm. The test was made twice quite independently in the same way. The stress-concentration factors* obtained by two tests are in close agreement except the case of $t/D=0.212$, as shown in Fig. 38, where filled circles give the results of the first test and open circles those of the second test. In every point, the second test was made with greater caution than the first test and the results are more reliable.

For comparison, Neuber's results also are shown in Fig. 38. The figure indicates that Neuber's analytical results are smaller than the experimental results herein obtained for $t/D>0.067$, but larger for $t/D<0.067$. Though the experimental results are for parallel-sided U-grooves and the analytical results are for hyperbolic-grooves, the discrepancy between the two are too large to attribute this to the difference of shapes of the two grooves.

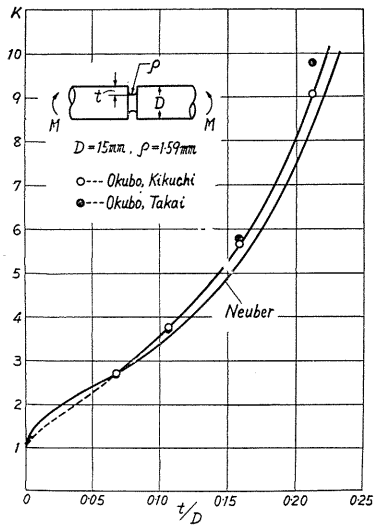

FIG. 38. Stress-concentration factors for shafts with circumferential U-groove, submitted to bending.

Having obtained the stress-concentration factor, the maximum stress σ_1 at the base of notch is found from the relation that

$$\sigma_1=\frac{32\,KM}{\pi D^3}, \tag{9}$$

where M is the bending moment acting on the specimen. If σ_2 and ε_2 represent the circumferential stress and strain at the base of notch, respectively, we have

$$\sigma_2=\nu\sigma_1+E\varepsilon_2, \tag{10}$$

where E and ν denote the Young's modu-

* Direct stress was used here for the criterion of producing flecks. On the surface of a specimen the maximum shearing stress is always one half of the largest principal stress, since the third principal stress vanishes there. Consequently, if the slight aeolotropy in the radial direction of the specimen, which may possibly exist in the plated copper by the process of deposition, be ignored, direct stress can be used for the criterion of flecking instead of shearing stress.

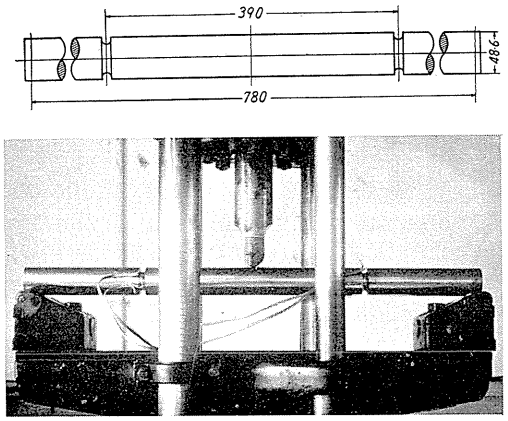

FIG. 39. Testing machine and dimensions of test piece in millimeter.

lus and the Poisson's ratio of the shaft, respectively.

The circumferential stress at the peak point is much smaller than the longitudinal stress, since its maximum value is only $\nu\sigma_1$, even in the limit case where the circumferential strain at the peak point is completely restrained by the neighbouring cylindrical portion of the shaft.

To examine the circumferential strain occurring at the peak point, a statical bending test was made using a shaft of mild steel with dimensions as shown in Fig. 39. A pair of notches of equal dimensions are cut at the symmetrical positions of the shaft. Circumferential strain at the peak points is measured by means of electric strain-gauges.

The Young's modulus of the steel is measured by bending at four symmetrical positions of the shaft before the machining of notches. The measured value of E is 2.05×10^6 kg/cm^2 and ν is assumed 0.28 for the steel. After the measurement of E, notches of smallest depth are cut at the locations shown in Fig. 39, and the circumferential strain is measured. The notches are accurately similar in shape to those employed for the examination of the longitudinal stress. After the measurement for notches of smallest depth, next notches of larger depth are cut and the circumferential strain for each notch is measured. The results obtained in this manner are given in Table 5.

To relieve the reduction of accuracy occurring from the unequality of individual strain-gauge, the circumferential strain is measured by using four strain-gauges placed at the peak points, two of which are active and the others

TABLE 5. Value of σ_2/σ_1, $D=48.6$ mm, $\rho=5.15$ mm

Depth of notch t (mm)	3.24	5.15	7.71	10.3
d/ρ	8.18	7.44	6.44	5.44
ε_2/M (10^{-8} kg^{-1} cm^{-1})	−1.00	−1.11	−1.39	−2.19
σ_1/M (cm^{-3})	0.241	0.335	0.504	0.806
σ_2/M (cm^{-3})	0.047	0.071	0.113	0.180
$R=\sigma_2/\sigma_1$	0.195	0.212	0.224	0.223

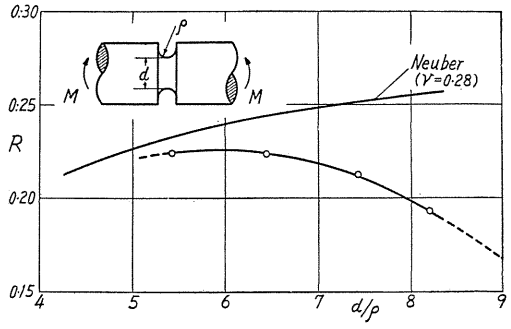

FIG. 40. Relation between R and d/ρ.

dummy. The values of σ_1 derived from (9), using the result shown in Fig. 38, are also given in Table 5. A curve showing the relation between the stress ratio σ_2/σ_1 and the minimum diameter of shaft d, is plotted in Fig. 40. As is shown in the figure, with increase of t, the stress ratio R rapidly increases first and attains the maximum value at a certain value of t, then gradually decreases as d approaches zero. This indicates that there exists the optimum depth of notch to restrain the circumferential strain at the base of notch, provided that D and ρ are prescribed.

The curve of R derived from Neuber's theoretical results for infinitely deep hyperbolic-notches are also given in Fig. 40. The two curves come close with each other as the depth of notch increases, namely the minimum diameter of the shaft approaches zero. This shows that the experimental results herein obtained is of sufficient accuracy, since experimental results for deep notches must agree with Neuber's theoretical results, if the difference in the shape of notches, parallelsided U-notch and hyperbolic notch, be ignored.

Strain Distribution in Metals

In engineering applications, the theory of elasticity based on the assumptions of homogeneity and isotropy is usually applied to metal structures. Metals are, however, far from being homogeneous when studied microscopically. The strain in a minute portion of a metal is not uniform even for a uniform tension member. Consequently, the validity of the theory is confined within a certain limit and the theoretical results can not be applied to a metal structure where the subject is the stress occurring in a minute area whose dimensions are not sufficiently large in comparison with those of the crystal grains constituting the metal.

The usual method of experimental strain-analysis is either incompetent or extremely laborious for the investigation of the microscopic strain distribution over a whole specimen of metal.

Recently the photostress method was applied by Kawada to examine the strain in an aluminium plate of large crystal grains submitted to tension and by Zandman to examine the strain around individual grains in a cold-drawn mild-steel strip submitted to torsion, respectively.[26]

The thickness of coating employed by the former is 1 mm which is about

centuple the thickness of plating usually employed for test. It is most essential, however, for an accurate determination of the irregular strain occurring in a minute area on the surface of a metal to have the possibly thinest coating. While the thickness of plating can be reduced even to a few microns. The measured value of strain by Zandman is of the order 2×10^{-2} which is about ten times the strain at yield point of a steel.

The photostress method may be useful for the qualitative determination of strain in a large crystal grain or of large plastic strain in metals but is almost incompetent for the accurate measurement of minute elastic strain, especilly for fine grained metals. While the electroplating method is favourably applied to such cases when the specimen under investigation can be submitted to reversals of cyclic stress. The method can be applied to a large metal structure as in the case of usual coatings, since a partial plating is possible.

Since the plated copper is very thin, the strain in the plated copper is just the same in the underlying metal, so the strain distribution in the underlying metal can be examined by observing the figure made by micro-flecks on the plated copper.

As an example, the strain figure on the plated copper for $(\alpha+\beta)$-brass are shown in Fig. 41. The specimens were cut from a cold-drawn wire. Micrographs of the flecks (*a*), the grown grains in the plated copper (*b*), and the constitution of the underlying brass (*c*), are shown in Fig. 42. Just beneath the portion where the flecking and the grain-growth are remarkable, the grains of α-phase are smaller in size but thicker in distribution in comparison with those of the neighbouring portion. The marked heterogeneity occurred in the material may be attributed to the process of cold-drawing.

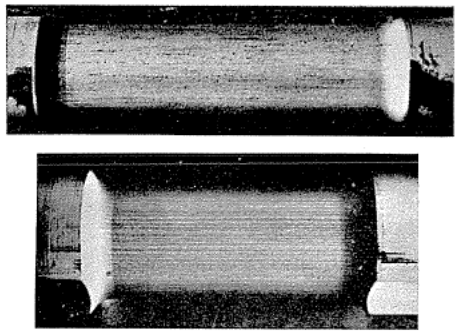

FIG. 41. Strain figures, basis metal of cold-drawn $(\alpha+\beta)$-brass; (*a*) bending, (*b*) torsion.

Even in the case of the cold-drawn wire, when the metal receives

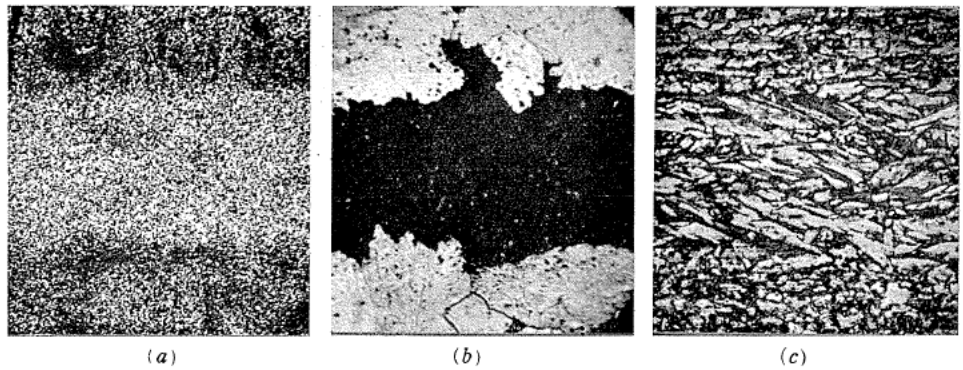

FIG. 42. (200×); (*a*) flecks, (*b*) grown-grains, (*c*) constitution of underlying $(\alpha+\beta)$-brass.

a suitable heat treatment, being homogeneous macroscopically, the strain figure as shown in Fig. 41 is not formed by fatigue.

Figure 43 shows the flecking on the plated copper for $(\alpha+\beta)$-brass rod received a suitable heat treatment. The micrograph of the constitution of the brass is shown in Fig. 44. As is shown in the figure, the grain size of the brass is about 0.03 mm. It is the same order of the grain size of the carbon steel used in this experiment.

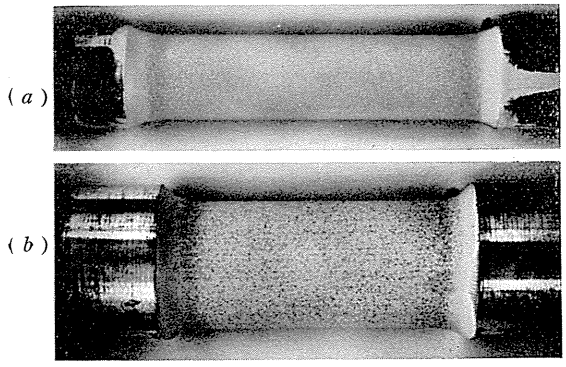

FIG. 43. Flecking, basis metal of cold-drawn $(\alpha+\beta)$-brass, annealed at 600°C; (*a*) bending, (*b*) torsion.

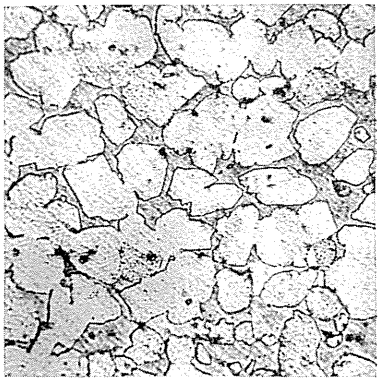

FIG. 44. Constitution of $(\alpha+\beta)$-brass, annealed, (280×).

Relation between strain and number of repetitions A preliminary test was made to find the relation between the proper value of shearing strain and the number of repetitions of cyclic stress. Conical rods of fine-grained carbon steel plated with copper, varied from 12 mm to 14 mm in diameter, Fig. 2, are used. Rotary bending test was made under a prescribed bending moment. For stepwise increasing repetitions of cyclic stress, the proper value of bending stress based on the underlying steel is obtained by measuring the length of the portion of a specimen changed in colour.

Since the maximum shearing stress in a uniform tension field is one half of the normal stress and the strains in the plated copper and the underlying steel are equal, the proper value of shearing strain in the plated copper is

$$\gamma = \frac{\sigma_x}{2G}, \tag{11}$$

where σ_x and G denote the normal stress and the modulus of rigidity of the basis metal, respectively.

Tests were made for the different loads, varied from 385 kg-cm to 595 kg-cm. The measured value of the modulus of rigidity of the steel is 8.2×10^3 kg/mm^2. From the experimental data thus obtained, a calibration curve, Fig. 45, showing the relation between the proper value of shearing strain γ and the number of repetitions of cyclic stress n is derived.

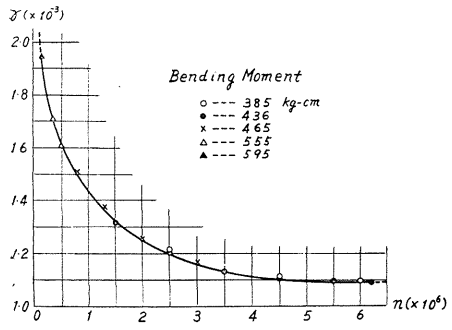

FIG. 45. Relation between proper value of shearing strain and number of repetitions of cyclic stress.

Strain distribution in α-brass

Tests were made to investigate the microscopic strain distribution in cylindrical rods of α-brass submitted to bending or torsion. Test pieces were cut from a cold-drawn wire which received heat treatment prior to machining so as to have equalized grains of different sizes, varied from 0.04 mm to 1.3 mm in average.

First, for the specimen of brass rod having the largest grain-size, namely 1.3 mm, the rotary bending test was made keeping the nominal bending stress constant, namely ± 8 kg/mm^2. The modulus of rigidity of the metal is 4.2×10^3 kg/mm^2. The test piece is a cylindrical rod of 13.2 mm diameter as shown in Fig. 47. The corresponding nominal shearing strain in the basis metal is

$$\gamma_0 = 0.95\times10^{-3}.$$

The surface of the specimen is carefully examined by microscope at stepwise increasing repetitions of the cyclic stress. The first flecks are observed at $n=1.5\times10^5$. By virtue of the curve in Fig. 45, the corresponding value of shearing strain is estimated to be 1.95×10^{-3}. This shows that the maximum shearing strain occurring in the brass rod is about 2.1 times the nominal strain. Typical strain figures for various numbers of repetitions of cyclic stress and the microscopic constitution of the underlying brass at the same location are shown in Fig. 46, where arrow lines indicate the axial direction of the specimen. As is shown in the figure, early flecks always appear along the grain boundaries of the basis metal in the direction of maximum shear and form lines having the length almost agrees with the grain size of the metal. The value of γ described indicates the shearing strain on the bounding curve of the flecked portion. The change of strain figure with advance of fatigue over the specimen is shown in Fig. 47.

At the place where early flecks appear, occurs remarkable change in constitution of the plated copper. Microscopic examination of the flecked portion, removed the flecked thin layer by electropolishing and etched, reveals the nature of grain growth in the plated copper. Typical figures are given in Fig. 48. The illustrations are the strain figure on the surface formed by flecking for $n=0.4\times10^6$ and the grain growth at the location revealed by electropolishing (a), the variation of the figure by an additional cyclic stress, namely for the total number of repetitions $n=1.2\times10^6$ and the figure revealed by the second electropolishing (b), the corresponding figures for $n=6\times10^6$ (c), and the microscopic constition of the basis metal at the same location (d), respectively. Minute observation on these figures suggests that some substance which causes the colour change originally mixed with the micrograins of the deposited copper is squeezed out to the surface of the plated copper with advance of grain growth. The large strain highly

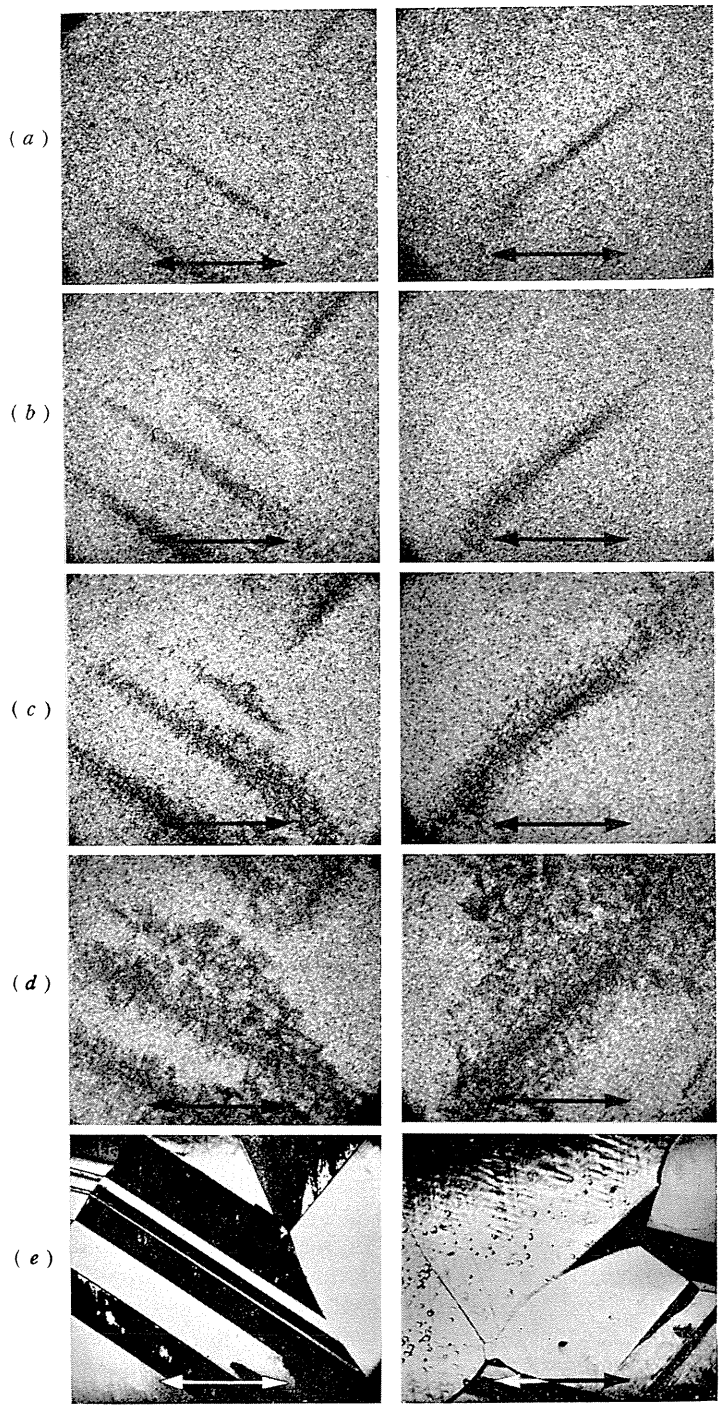

FIG. 46. Micrographs of figures showing the strain distribution in rotary bending, (35×); (*a*) $\gamma=1.80\ \gamma_0$, (*b*) $\gamma=1.60\ \gamma_0$, (*c*) $\gamma=1.40\ \gamma_0$, (*d*) $\gamma=1.15\ \gamma_0$, (*e*) constitution of α-brass.

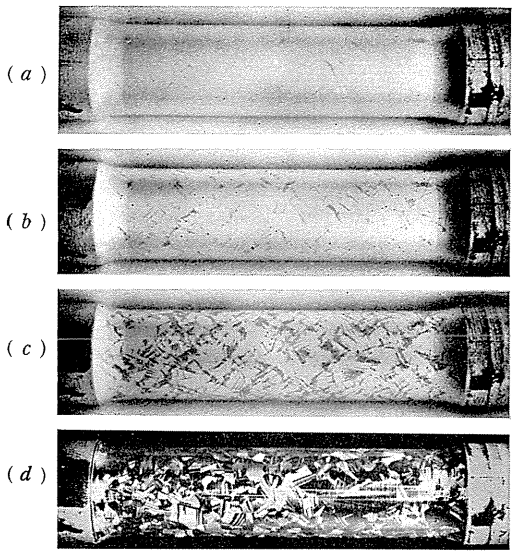

FIG. 47. Change of strain figure with advance of fatigue, rotary bending; (*a*) $n=0.7\times10^6$, (*b*) $n=1.5\times10^6$, (*c*) $n=6\times10^6$, (*d*) constitution of α-brass.

concentrated along the grain boundary of the basis metal causes, in some instances, a crack in the plated copper as shown in Fig. 48 (*b*), (*c*), though the basis metal suffers no change.

A similar test for torsion is made using a specimen of the same material, diameter of which is 12.8 mm, for the nominal shearing stress of ±4.0 kg/mm^2. The nominal shearing strain in torsion is

$$\gamma_0=0.95\times10^{-3}.$$

The first flecks are observed at $n=2\times10^5$, and the corresponding shearing strain estimated from the curve in Fig. 45 is 1.85×10^{-3}. This shows that the maximum strain in torsion occurring in the basis metal is 1.95 times the nominal strain. The micrographs of the strain figure showing the strain distribution near a grain boundary and the microscopic constitution of the underlying brass at the same location are given in Fig. 49. The change of strain figure in torsion with advance of fatigue is shown in Fig. 50. The change in constitution occurring in the plated copper with advance of fatigue is shown in Fig. 51.

In torsion, lines of flecks appearing along the grain boundaries of the basis metal are in the directions, either parallel or perpendicular to the axis of the specimen. This shows that both in torsion and bending early flecks always form lines in the directions of maximum shear.

Next, a similar test was made for the brass rod having moderate grain-size, namely 0.45 mm in average. The result and the conclusion introduced therefrom are quite similar to those of the preceding test, but the maximum shearing strain occurring in a rod is perceptively reduced in magnitude both in bending and torsion. The maximum shearing strain derived in the same manner is 1.8 and 1.7 times the nominal shearing strain for bending and torsion, respectively. The micrographs of strain figures showing the strain distribution around a grain boundary and the constitution of the underlying brass at the same location are given for rotary bending and torsion in Figs. 52 and 53, respectively.

The change in constitution occurring in the plated copper with advance of fatigue is shown in Figs. 54 and 55. These figures for the grain size 0.45 mm correspond to Figs. 48 and 51 for the grain size 1.3 mm.

Figure 56 shows the lines of equi-shearing-strain around grain boundaries derived from Figs. 46, 49, 52 and 53, respectively. Dashed lines are the boundaries of the crystal grains in α-brass.

When the grain size of the brass is quite small, the strain figure described

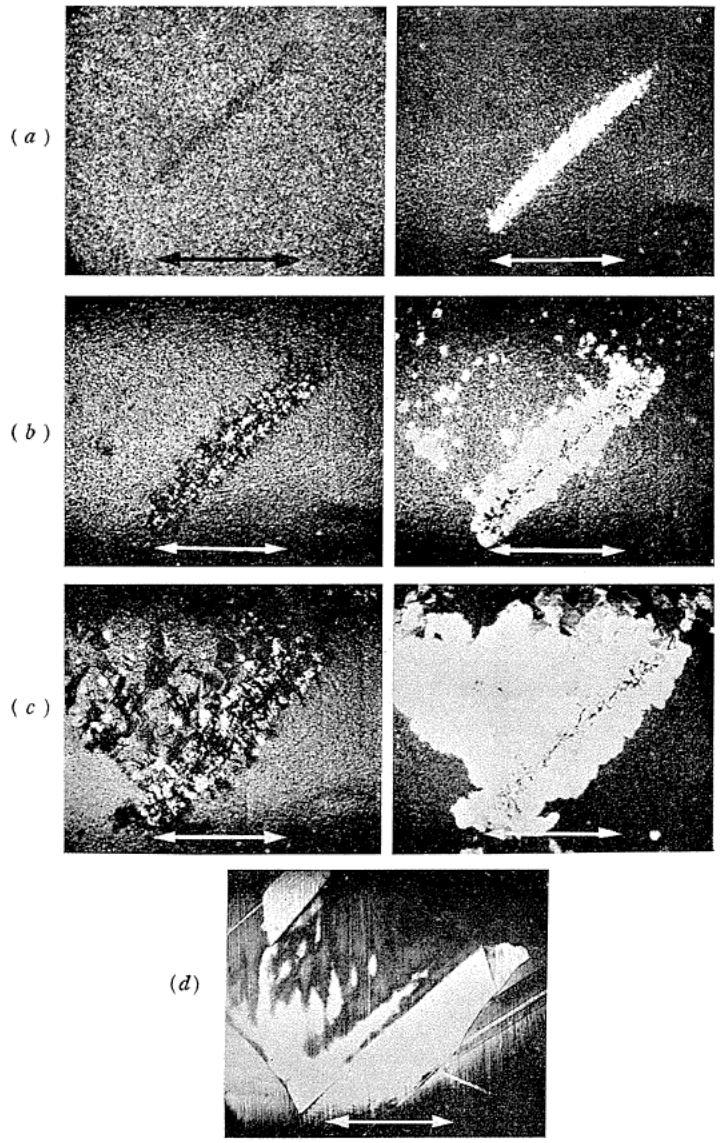

FIG. 48. Change of constitution in plated copper with advance of fatigue, rotary bending, (35×); (*a*) $n=0.4\times10^6$, (*b*) $n=1.2\times10^6$, (*c*) $n=6\times10^6$, (*d*) constitution of α-brass.

is not formed by flecking, as is shown in Fig. 57. Since the strain concentration along the grain boundaries is not so intense as in the case of large grain-size, and since flecking, in general, occurs only when large grown-grains of the order of 0.1 mm are produced in the plated copper, little can be detected regarding the strain concentration along the grain boundaries by mere observation of flecking.

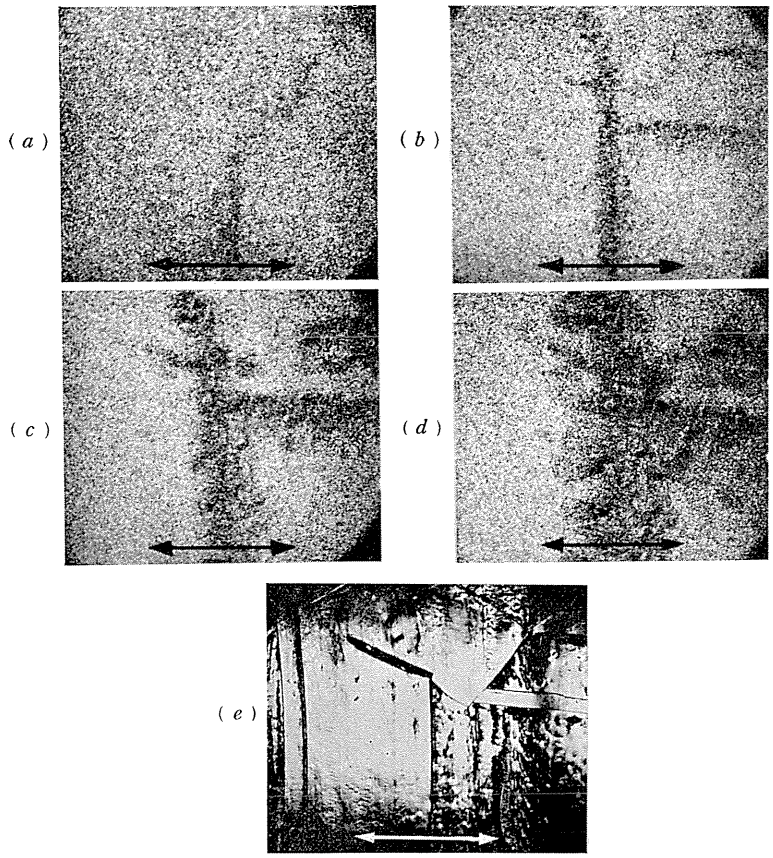

FIG. 49. Micrographs of figures showing the strain distribution in torsion, (35×); (*a*) $\gamma=1.80\ \gamma_0$, (*b*) $\gamma=1.56\ \gamma_0$, (*c*) $\gamma=1.28\ \gamma_0$, (*d*) $\gamma=1.15\ \gamma_0$, (*e*) constitution of α-brass.

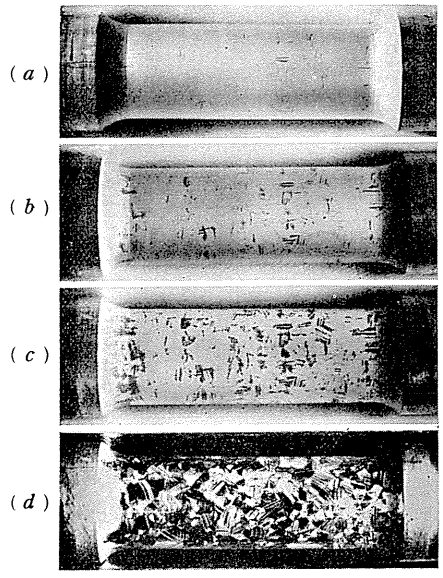

FIG. 50. Change of strain figure with advance of fatigue, torsion; (*a*) $n=0.85\times10^6$, (*b*) $n=2.3\times10^6$, (*c*) $n=6\times10^6$, (*d*) constitution of α-brass.

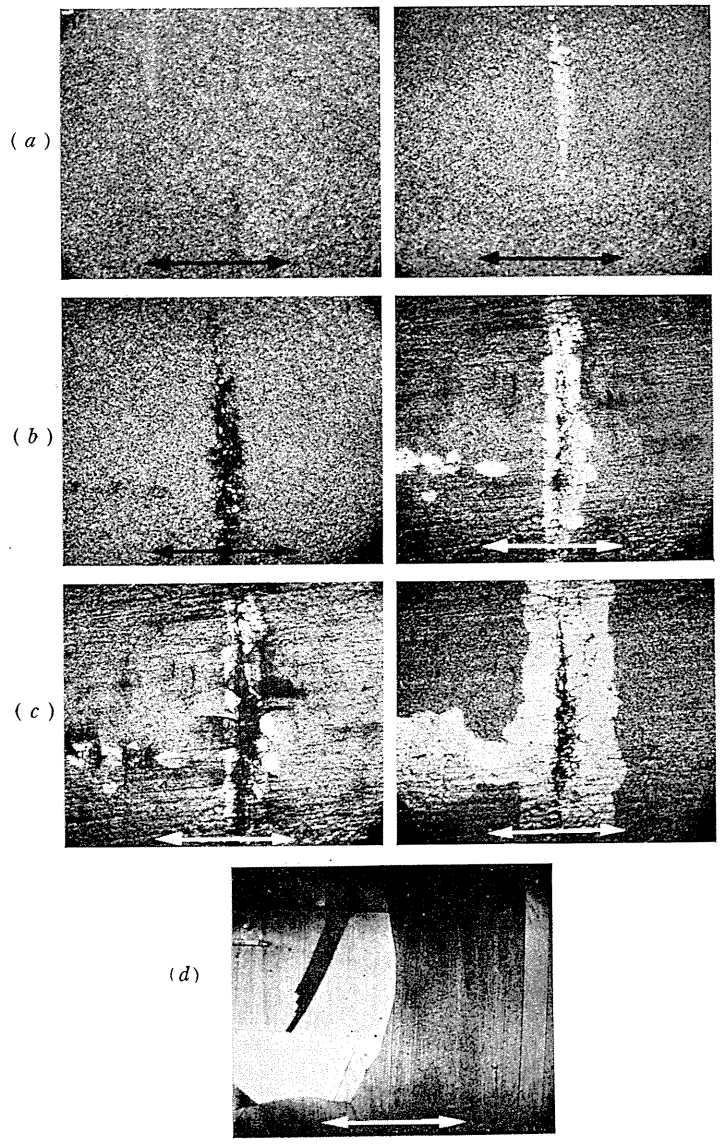

FIG. 51. Change of constitution in plated copper with advance of fatigue, torsion, (35×); (*a*) $n=0.5\times10^6$, (*b*) $n=1.7\times10^6$, (*c*) $n=6\times10^6$, (*d*) constitution of α-brass.

The size of grown-grain is, however, only a few microns at the early stage of occurrence, so the irregular strain in a minute area in metals is easily found by observing the grain growth occurring in the plated copper.

Close examination of grain growth reveals the strain concentration along the grain boundaries even for the metals of the grain-size 0.04 mm, the smallest one examined in this experiment. The strain concentrates along the grain boundaries

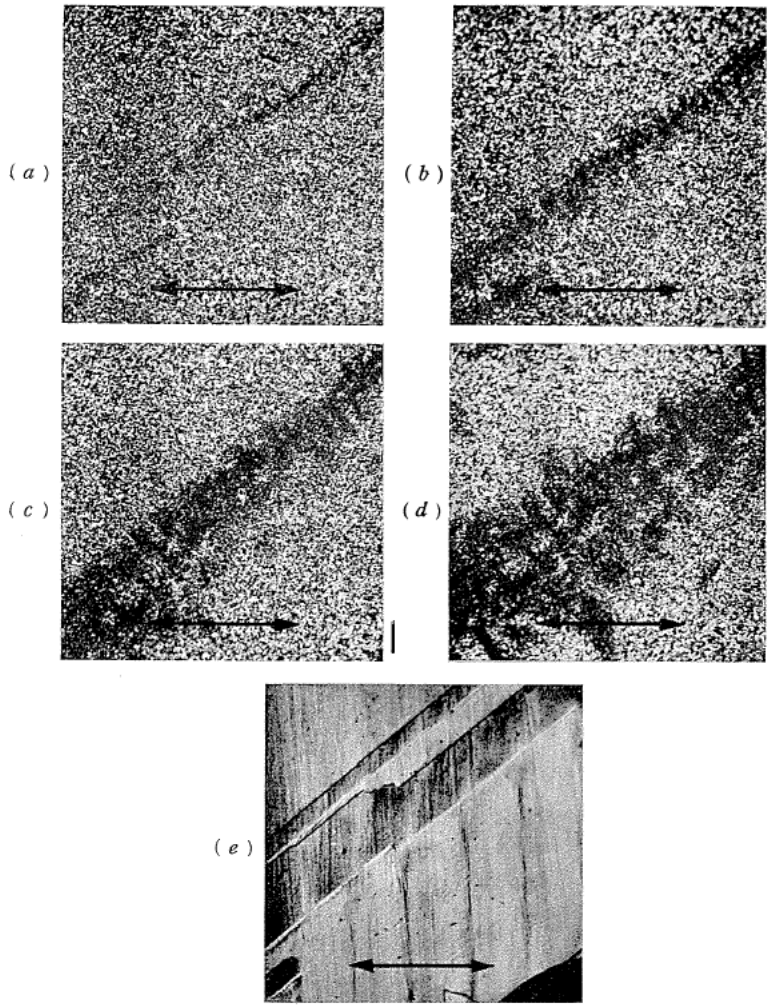

FIG. 52. Micrographs of figures showing the strain distribution in rotary bending, (65×); (*a*) $\gamma=1.75\ \gamma_0$, (*b*) $\gamma=1.56\ \gamma_0$, (*c*) $\gamma=1.34\ \gamma_0$, (*d*) $\gamma=1.19\ \gamma_0$, (*e*) constitution of α-brass.

in the directions of maximum shear as in the case of large grain-size. Figs. 58-64 are illustrations showing the early status of grain growth occurred at the grain boundaries of the basis metals, and the constitution of the metals at the same locations. The averaged value of grain size of the carbon steel is 0.04 mm and that of the α-brass 0.09 mm and 0.04 mm, respectively. The fact that grain growth occurs, in many instances, over the whole area of a grain at the early stage of test, Fig. 64, indicates that the strain at the grain boundary is not much larger than the one within the crystal and that the strain within individual grains is almost uniform. This leads to an important conclusion pertaining the fatigue failure of metals that the stress distribution in a specimen may be

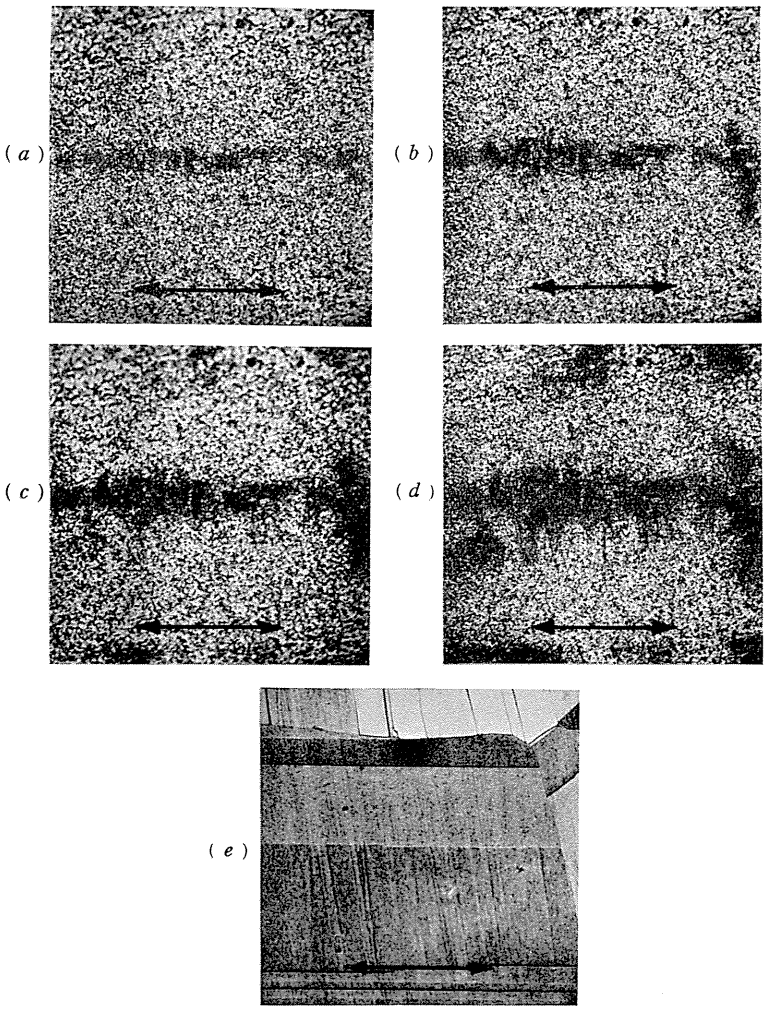

FIG. 53. Micrographs of figures showing the strain distribution in torsion, (65×); (*a*) $\gamma=1.54\,\gamma_0$, (*b*) $\gamma=1.33\,\gamma_0$, (*c*) $\gamma=1.21\,\gamma_0$, (*d*) $\gamma=1.12\,\gamma_0$, (*e*) constitution of α-brass.

irregular but it is almost uniform at least in individual crystal grain when the grain size is sufficiently small. This tends to hold the assumption upon which Neuber introduced his new theory on notches with minute base radius and also some subsequent experimental results based on his theory.[27]

A curve showing the relation between the maximum shearing strain and the grain size of the α-brass is obtained from the results based on the observation of flecking and is given in Fig. 65.

In bending and torsion, slip bands can hardly be found on the surface of the brass within the load employed in the tests described, either statical or dynamical. This indicates that the lines of flecks which appear at the early stage of the test

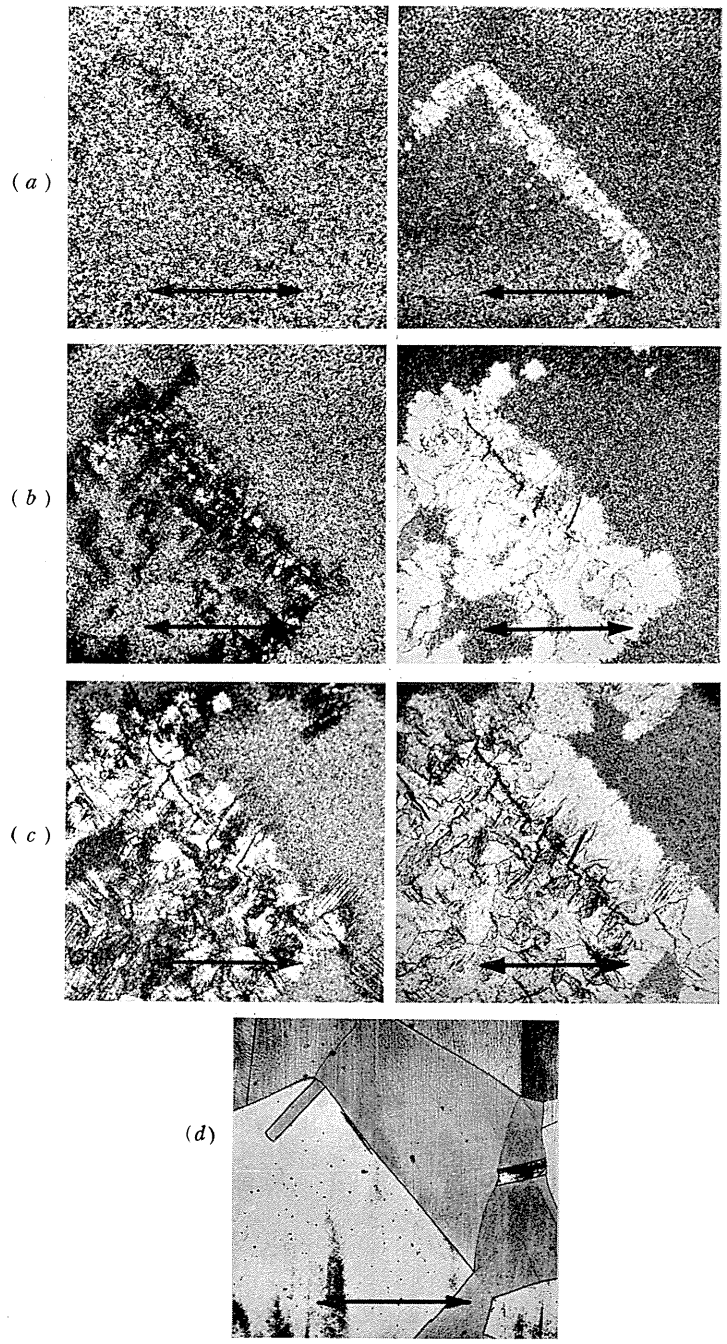

FIG. 54. Change of constitution in plated copper with advance of fatigue, rotary bending, (65×); (*a*) $n=0.6\times10^6$, (*b*) $n=1.8\times10^6$, (*c*) $n=6\times10^6$, (*d*) constitution of α-brass.

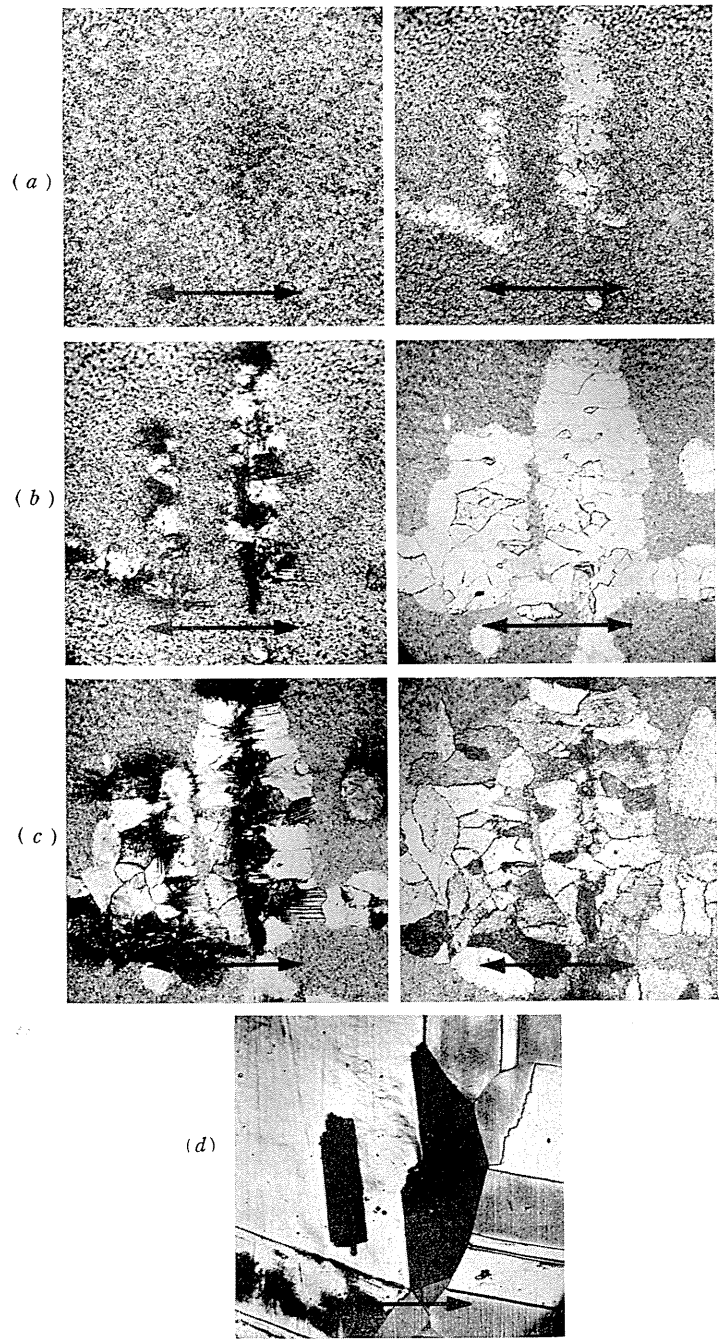

FIG. 55. Change of constitution in plated copper with advance of fatigue, torsion (65×); (*a*) $n=0.8\times10^6$, (*b*) $n=2.2\times10^6$, (*c*) $n=6\times10^6$, (*d*) constitution of α-brass.

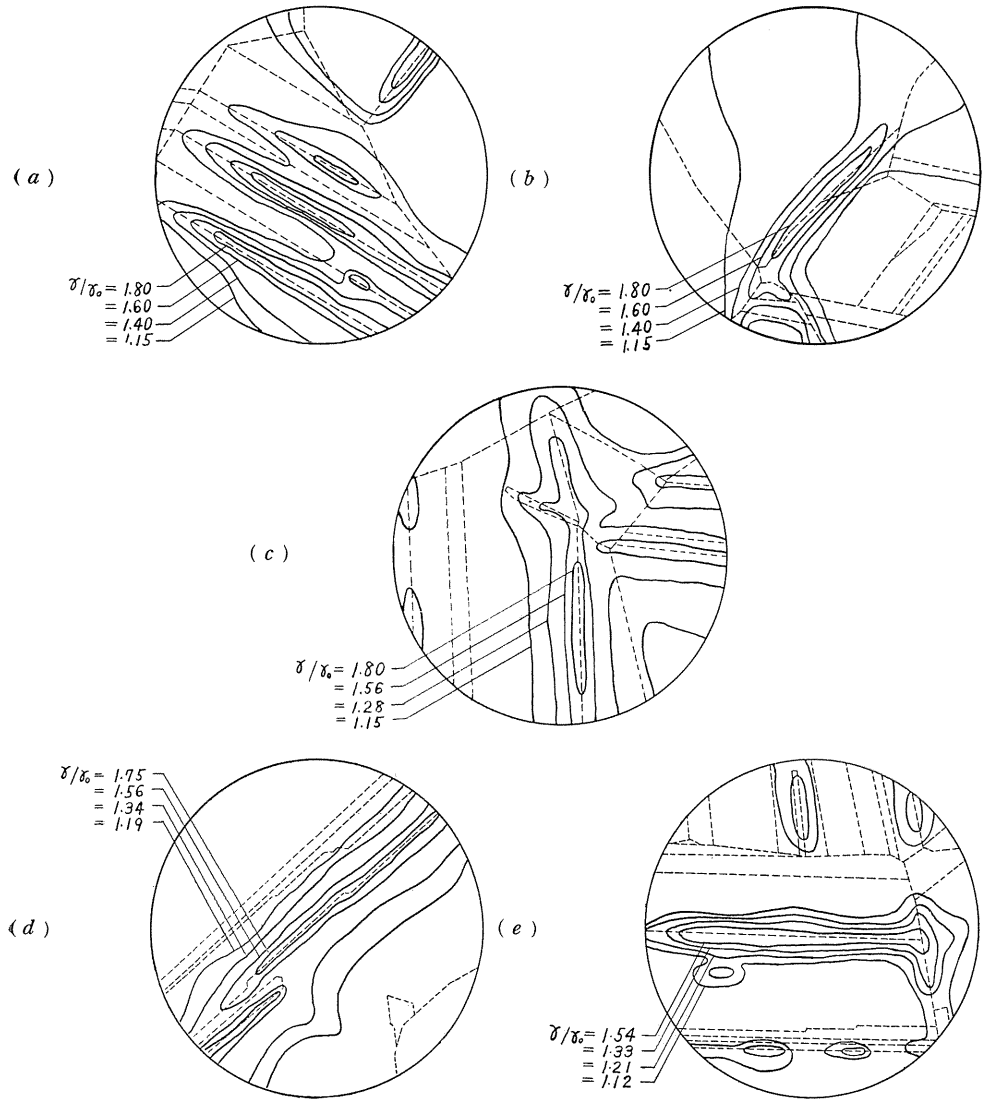

FIG. 56. Lines of equi-shearing-strain around grain boundary; at the locations shown in Fig. 46, (*a*), (*b*); Fig. 49, (*c*); Fig. 52, (*d*); Fig. 53, (*e*).

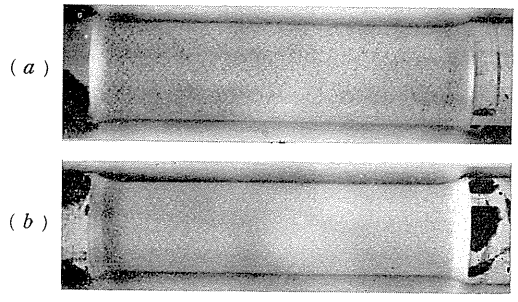

FIG. 57. Flecking, (*a*) grain size 0.09 mm, (*b*) grain size 0.04 mm.

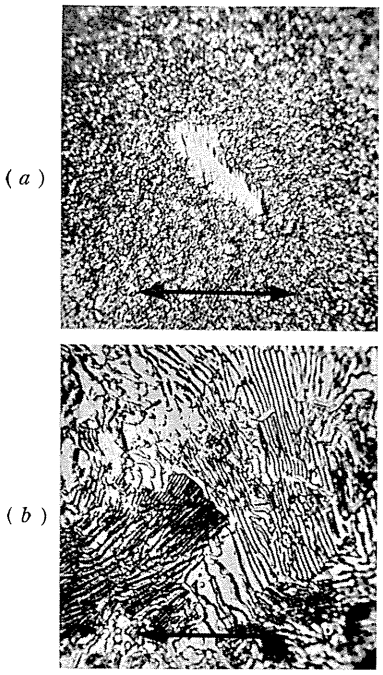

FIG. 58. Grain growth (*a*), and the constitution of underlying carbon steel (*b*), grain size 0.04 mm, rotary bending (660×).

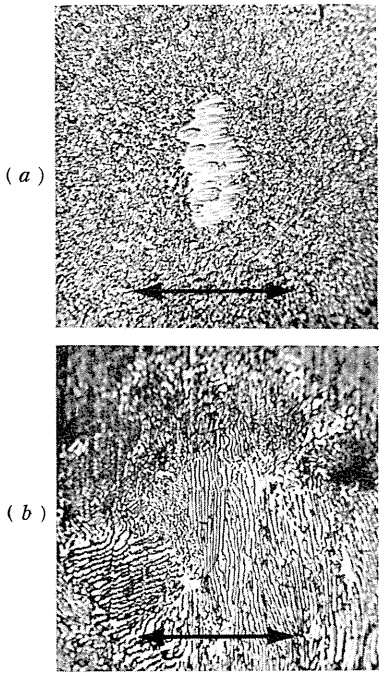

FIG. 59. Grain growth (*a*), and the constitution of underlying carbon steel (*b*), grain size 0.04 mm, torsion (660×).

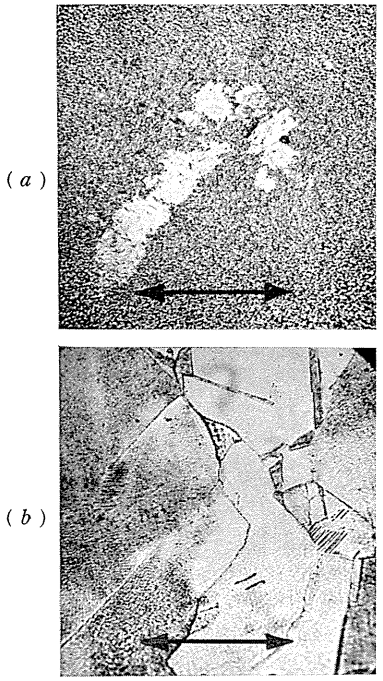

FIG. 60. Grain growth (*a*), and the constitution of underlying α-brass (*b*), grain size 0.09 mm, rotary bending (230×).

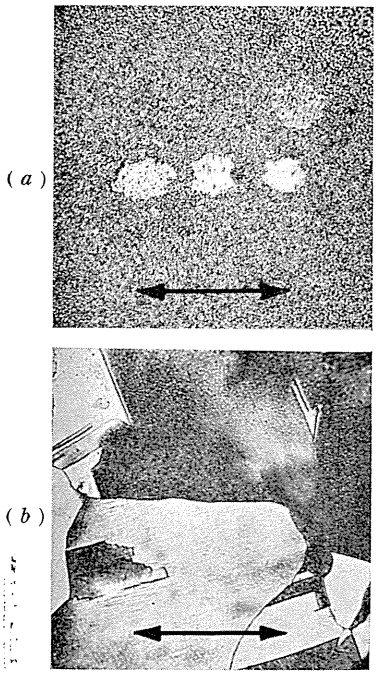

FIG. 61. Grain growth (*a*), and the constitution of underlying α-brass (*b*), grain size 0.09 mm, torsion (230×).

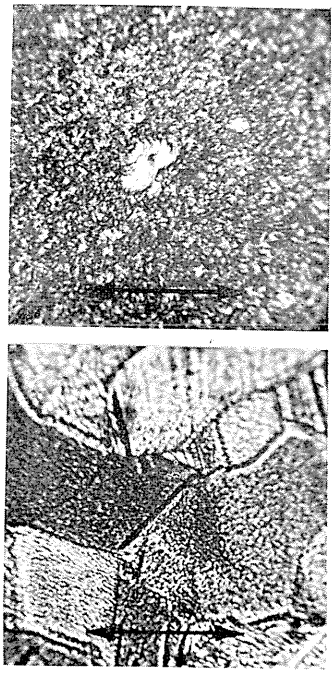

FIG. 62. Grain growth (*a*), and the constitution of underlying α-brass (*b*), grain size 0.04 mm, rotary bending (660×).

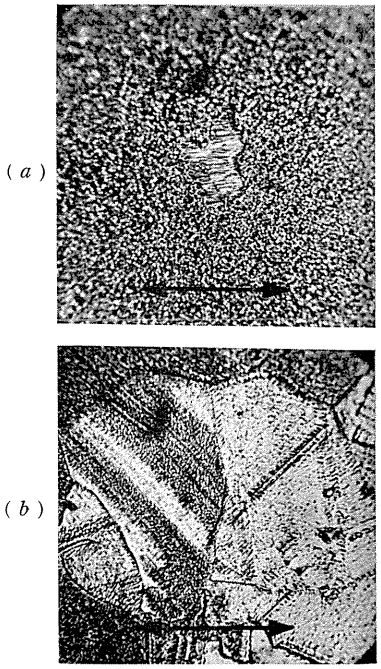

FIG. 63. Grain growth (*a*), and the constitution of underlying α-brass (*b*), grain size 0.04 mm, torsion (660×).

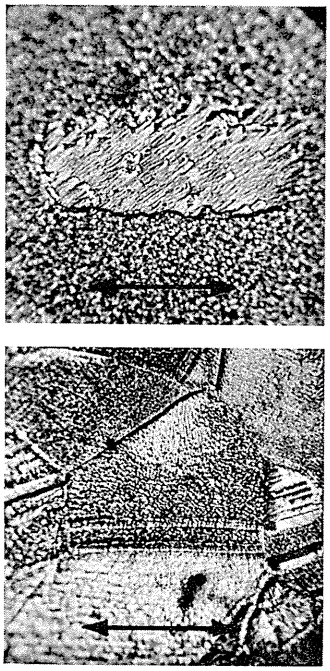

FIG. 64. Grain growth (*a*), and the constitution of underlying α-brass (*b*), grain size 0.04 mm, torsion (660×).

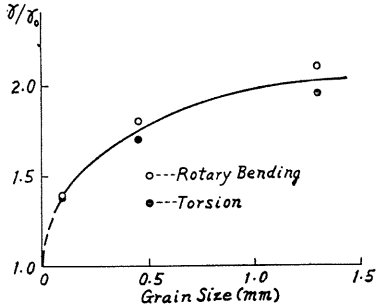

FIG. 65. Relation between the maximum strain and the grain size of α-brass.

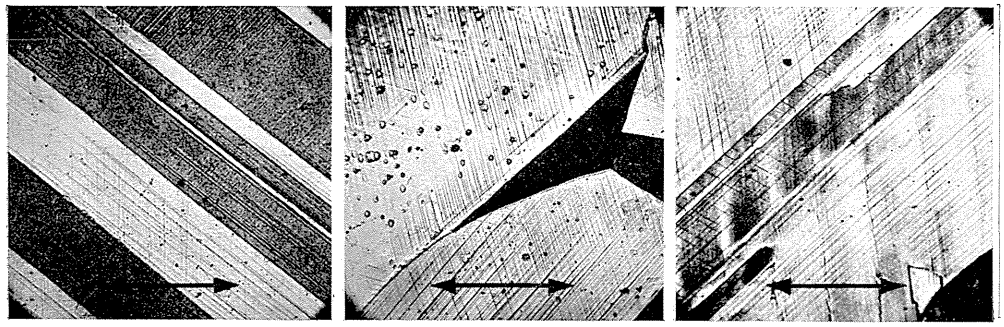

FIG. 66. Slip bands produced by statical tension-test at the locations shown in Fig. 46 (*e*), (60×) and Fig. 52 (*e*), (60×).

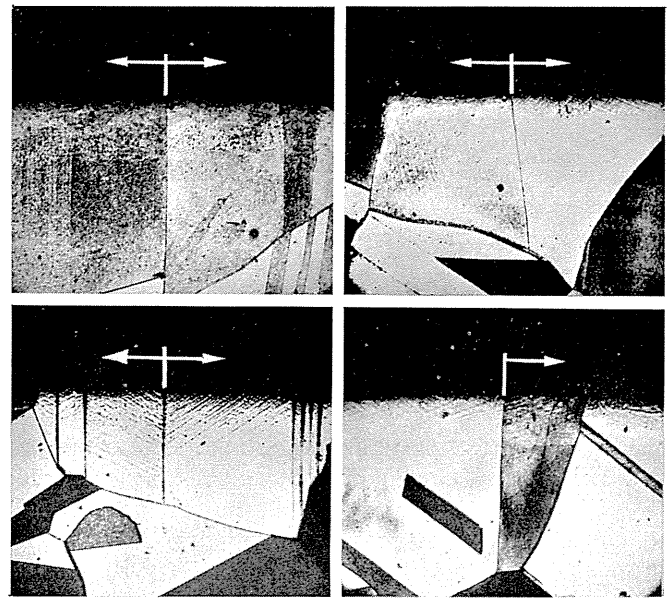

FIG. 67. Cross sectional view of the boundary-plane where strain highly concentrates.

are not figures expressive of slip bands formed in the underlying brass and that if admitted a small slip within a crystal grain, the strain at the grain boundary is much larger than the strain within the crystal.

In statical tension test, however, slip bands are formed for the stress employed in the rotary bending test. Fig. 66 is the micrographs of the slip bands produced by statical tension test at the same locations shown in Figs. 46 (*e*) and 52 (*e*). It is seen from the figure that the directions of slip planes of the adjacent crystal grains are perceptively different at the grain boundary where early flecks appeared.

Examination of the cross section of specimens at the location where early flecking occurs reveals that the boundary-plane of crystal grains in the basis

brass always cut the surface of the brass almost at right angles, as is illustrated in Fig. 67. This shows that the boundary-plane where highly concentrated strain occurs is a plane of maximum shear perpendicular to the surface of the specimen. Arrow lines in the figure indicate the direction of advance of flecking with increase of n. The figure also indicates that the strain concentrates more intensely at the boundary-plane of larger crystal grains.

It is known that the layer first deposited has a microstructure similar to that of the basis metal when the surface is very clean.[28] But after all microscopic examination of the cross section of a specimen before stressing, any preferred orientation showing the influence of the microstructure of the basis metal can not be observed in the deposited copper. Consequently the strain figure described are entirely attributed to the irregularity of the strain distribution in the basis metal and not to the original microstructure of the deposited copper.

The experimental results herein obtained lead to the conclusion that the shearing strain is considerable at the grain boundaries in the directions of maximum shear, especially when the slip planes of the adjacent crystal grains greatly differ in orientation. When the grain size is comparatively large, the maximum shearing strain is almost twice the magnitude of the nominal strain derived from the theory of elasticity, but with decrease of grain size the strain concentration at grain boundaries is gradually relieved. For the α-brass with equalized grains of comparatively large size, the early flecks always form lines in the directions of maximum shear. But after excessive repetitions of cyclic stress, the strain figure does not always indicate the directions of maximum shear.

Promising Field of Application

The promising application of the method in future is the prediction for the fatigue failure which may occur in machine elements and structures submitted to reversals of cyclic stress in working state. But for this purpose, it is required that the plated copper maintains constant in quality during a long interval for observation. As was described, however, the lapse of time after the deposition has little effect on the value of proper stress and this is true even for the lapse of more than a year.[11] This favourable character of the plated copper makes it easy to apply the method to predict the failure of machines and structures in practice.

The method is also applicable to locate the peak points in a machine element when the element vibrates in running state, even when the external force acting on the element, the intensity and mode of vibration are not ascertained. This often occurs for a machine element rotating in a closed casing. In such a case, the peak points can not be found otherwise until the element breaks down. One example will be shown. Fig. 68 is the skeleton view of the rotating part of a stepless speed-regulator. The fatigue failure of flanged disks occurs in some instances, since rotating disks in a closed casing are set in vibration by some obscure causes. Typical modes of failure caused by fatigue are shown in Fig. 69. Fig. 70 are micrographs of grain-growth showing the stress concentration at the peak points of a flanged disk, namely at corners of

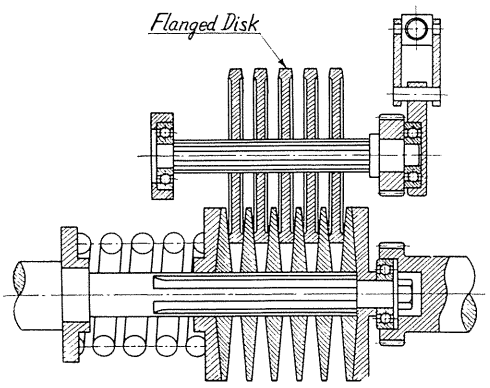

FIG. 68

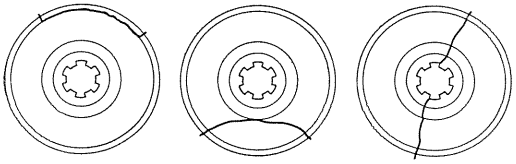

FIG. 69

FIG. 68. Rotating part of a stepless speed-regulator.

FIG. 69. Typical modes of fatigue failure in flanged disks.

FIG. 70. Micrographs of grain growth; (*a*) location of peak points, (*b*) edge of spline, (*c*) sharp corner of flange, (*d*), (*e*) round corner of flange.

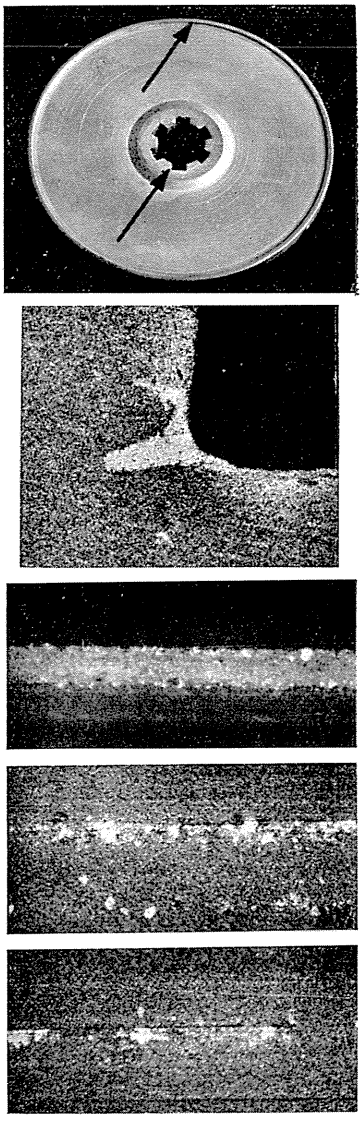

FIG. 70

flange (*c*), (*d*), (*e*) and spline (*b*). The illustration apparently shows the large stress highly concentrated at the sharp corner of flange (*c*), and the relieved stress at the round corner of flange (*d*), (*e*).

Conclusion and Remarks

The outline of the cause of flecking and the factors controlling the proper stress was described. But the mechanism of the flecking and the substance which causes the chemical change creating the flecks have not been ascertained. It is concluded, however, that the chemical change is due to some substance

contained in the plated copper and not to oxygen in the atmosphere. This is verified by the fact that, when a specimen is isolated from the air by a coating of vinyl prior to stressing, it changes as usual in colour while there is no discernible change in the appearance of flecks.

The change of temperature in the plated copper caused by cyclic stress is measured by means of electric strain-gauges. The temperature rise begins when the magnitude of the cyclic stress reaches the proper stress, but amounts to only several degrees even for stressing in considerable excess above the proper stress. It is concluded that such a small temperature rise cannot be the cause of grain growth, which then must be attributed to a pure mechanical cause, namely the reversals of cyclic shearing strain.

Except the case where the relevant theoretical result of sufficient accuracy is not available, it is ascertained that the experimental results for the stress-concentration factors in shafts found by the method are in good agreement with every known theoretical value or theoretically presumed value. This excellent agreement between the experimental and theoretical results indicates that the electroplating method of stress analysis can be applied to similar problems with sufficient accuracy.

A handy method of measuring the strain distribution in metals is presented. A similar procedure is already applied by Suzuki to the determination of stress distribution in a shaft containing a large transverse hole and submitted to torsion.[6] The method is applied to α-brass having equalized grain-size, dimensions of which vary from 0.04 mm to 1.3 mm in average. The results for cylindrical shafts of α-brass submitted to torsion or bending all indicate the high strain-concentration at the grain boundaries in the directions of maximum shear. The strain-concentration, however, is greatly relieved when the grain size is quite small.

The author suggests the applications of the method which will be developed in future. But for an accurate prediction of fatigue failure in machines or structures in working, there is required the quantitative determination of peak stress. For this purpose, an extensive investigation must be carried out on the nature of flecking, such as the variation of proper stress by an elevatated temperature during test, the effect of combined steady and cyclic stresses, etc.

A complete list of publications concerning the electroplating method is given chronologically. But so far as the author is aware, no information from foreign scientists is available.

Acknowledgement

It is a pleasure for the author to express his thanks to Mr. S. Satō, Assistant, Tōhoku University and to Mr. K. Hosono, Assistant, Nagoya University, for their earnest help in carrying out this investigation. A greater portion of this paper is taken in essence from the dissertations by K. Takai, N. Nozaki, S. Kikuchi and T. Suzuki presented respectively to the Faculty of Engineering, Nagoya University, in partial fulfilment of the requirements for the degree of Master of Engineering.

Thanks are also due to the Ministry of Education of Japan for their Grant-in-Aid for Fundamental Science Research.

Bibliography

1) Ōkubo, H. *Kikai no Kenkyū*, **5**, 1953, p. 663, **6**, 1954, p. 191, **7**, 1955, p. 514, **9**, 1957, p. 371, p. 469, **10**, 1958, p. 971, **11**, 1959. p. 641, (in Japanese).
2) Ōkubo, H. Determination of the Surface Stress by Means of Electroplating. *J. App. Phys.*, **24**, 1953, p. 1130.
3) Ōkubo, H. Stress-Concentration Factors for a Circumferential Notch in a Cylindrical Shaft. *Memoirs of the Faculty of Engineering, Nagoya Univ.*, **6**, 1954, p. 23.
4) Ōkubo, H. and Satō, S. Stress-Concentration Factors in Shafts With Transverse Holes as Found by the Electroplating Method. *J. App. Mech., Trans. ASME*, **22**, 1955, p. 193.
5) Ōkubo, H. and Takai, K. Stress-Concentration Factors in Shafts Containing Transverse Holes and Subjected to Bending. *J. App. Mech., Trans. ASME*, **23**, 1956, p. 478.
6) Suzuki, M. Determination of the Distribution of Maximum Shearing Stress on Metal Surfaces by Means of Electroplating Method. *Proc. 6th Japan National Congress for App. Mech.*, 1956, p. 103.
7) Suzuki, M. Strain Figures Appearing on the Surface of Copper Electrodeposits Subjected to Fatigue. *J. Inst. Metals*, **85**, 1956–57, p. 206.
8) Ōkubo, H. and Kikuchi, S. Stress-Concentration Factors in Shafts. *J. App. Mech., Trans. ASME*, **24**, 1957, p. 313.
9) Ōkubo, H. and Nozaki, N. Grain-Growth in Metals by Cyclic Stress. *Nature*, **180**, 1957-Sept., p. 604. Grain-Growth and Flecking in Electroplated Copper Caused by Cyclic Stress. *J. Electrochemical Soc.*, **105**, 1958, p. 384.
10) Suzuki, M. Über die Entstehung der Flecken an der Oberfläche von kathodischen Kupferniederschlägen bei Wechselbeanspruchung. *Z. Metallkde*, **48**, 1957, p. 395.
11) Satō, Y. and Morikawa, K. On the Measurement of Repeated Stress by Means of Electroplating. *Zairyō Shiken*, 8, 1959, p. 161 (in Japanese).
12) Thompson, N., Wadworth, N. and Louat, N. *Phil. Mag.*, **1**, 1956, p. 113.
13) Neuber, H. *Kerbspannungslehre*, Julius Springer, Berlin, 1958. p. 60.
14) Seely, F. B. and Dolan, T. J. *Univ. Illinois Eng. Exp. Station Bulletin*, No. 276, 1935.
15) Thum, A. and Kirmser, W. *VDI Forschungsheft*, No. 419, March-April, 1943. Seeger, G. *Die Technik*, **3**, 1948, p. 308. *Engineers Digest*, February, 1949, p. 51.
16) Peterson, R. E. and Wahl, A. M. *J. App. Mech., Trans. ASME*, **58**, 1936, p. A-15. Frocht, M. M. *J. App. Mech., Trans. ASME*, **66**, 1944, p. A-10. Heywood, R. B. *Designing by Photoelasticity*, Chapman and Hall, London, 1952.
17) Sonntag, R. *Z. angew. Math. Mech.*, **9**, 1929, p. 3. Neuber, H. *loc. cit.* p. 147. Ōkubo, H. *J. App. Mech., Trans. ASME*, **19**, 1952, p. 16. *A Handbook on Torsional Vibration, B.I.C.E.R.A.*, Cambridge Univ. Press, 1958, p. 330.
18) Willers, F. A. Z. *Math. Phys.*, **55**, 1907, p. 251.
19) Ōkubo, H. *J. App. Mech., loc. cit.*
20) Jacobsen, L. S. *Trans. ASME*, **47**, 1925, p. 619.
21) Lipson, C., Noll, G. C. and Clock, L. S. *Stress and Strength of Manufactured Parts*, McGraw-Hill Book Company, Inc., New York, 1950, p. 65. *Design Data and Methods, App. Mech., ASME*, 1953, p. 61. *Handbook on Mechanical Engineering, JSME*, 1951, p. 4–100 (in Japanese).
22) Leven, M. M. Quantitative Three-Dimensional Photoelasticity. *Scientific Paper 60-94459-2-P 1, Westinghouse Research Laboratories.*
23) Jessop, H. T. *J. Roy. Aero. Soc.*, **57**, 1953, p. 125.
24) Frocht, M. M., Guernsey, R. Jr. and Landsberg, D. *J. App. Mech., Trans. ASME*, **19**, 1952, p. 124.
25) Isida, M. On the Tension of the Strip with Semicircular Notches. *Trans. Japan Soc. Mech. Engrs.* **19**, 1953, p. 5 (in Japanese).
26) Kawada, K. *Reports Inst. Phys. Chem. Res.*, **34**, 1958, Abstract No. 63.
Zandman, F. Pick off Stress Data from Photomicrograph. *Product Engineering*, March 2, 1959, p. 21.

27) Neuber, H. *loc. cit.* p. 165. Minamiōzi, K. and Ōkubo, H. *J. Franklin Institute*, **249**, 1950, p. 49. Ōkubo, H. *J. App. Phys.*, **21**, 1950, p. 1105.
28) Gray, A. G. *et al.* *Modern Electroplating*, John Wiley and Sons, Inc., New York, 1953, p. 27.